Title
STUDIES IN TERRESTRIAL GAMMA RADIOACTIVITY

Authors
Wollenberg, Harold A.
Smith, Alan R.

Publication Date
1963-04-12

UCRL-10636

University of California

Ernest O. Lawrence Radiation Laboratory

STUDIES IN TERRESTRIAL GAMMA RADIOACTIVITY

Berkeley, California

UCRL-10636

UNIVERSITY OF CALIFORNIA

Lawrence Radiation Laboratory
Berkeley, California

Contract No. W-7405-eng-48

STUDIES IN TERRESTRIAL GAMMA RADIOACTIVITY

Harold A. Wollenberg and Alan R. Smith

April 12, 1963

STUDIES IN TERRESTRIAL GAMMA RADIOACTIVITY

Contents

UCRL-10636

STUDIES IN TERRESTRIAL GAMMA RADIOACTIVITY

Harold A. Wollenberg and Alan R. Smith

Lawrence Radiation Laboratory
University of California
Berkeley, California

April 12, 1963

ABSTRACT

In a search for cement and aggregate materials low in radioactivity for low-background shielding concrete, we have accumulated substantial data on the natural radiation environment. Our methods incorporate field measurement of the gamma radioactivity of various rock types by means of a portable scintillation counter utilizing a 3- by 3-in. NaI(Tl) crystal. Rock and soil samples are collected and, upon return to the laboratory, their gamma activities are studied with a 100-channel pulse-height analyzer (PHA).

Mathematical techniques in the form of IBM-7090 computer codes are applied to the PHA data, yielding the concentrations of K, U, and Th in the analyzed samples; in addition, we obtain the contribution of fission-product fallout to each gamma-ray spectrum. Correlation between field measurements and laboratory analyses are discussed; the serious complications to both posed by recent fallout are described. Results of K, U, and Th analyses are given for basaltic, ultramafic, carbonate, and quartziferous rock types. The results of a study of the radioactivities of portland-cement raw materials and finished products, and a possible correlation between the radioactivities of cements and their source limestones in the U. S. are discussed.

A knowledge of K, U, and Th concentrations can be of great value to the earth scientist; proposed applications include (a) determining the flow of heat in the earth's crust, (b) establishing the temperature conditions at which rocks have undergone regional metamorphism, and (c) determining possible correlations between the amount of K-feldspar and the concentrations of U and Th in Jurassic and Cretaceous sandstones in California.

STUDIES IN TERRESTRIAL GAMMA RADIOACTIVITY*†

Harold A. Wollenberg and Alan R. Smith

Lawrence Radiation Laboratory
University of California
Berkeley, California

April 12, 1963

INTRODUCTION

Our studies of terrestrial gamma-radiation were motivated by a specific problem: to determine the most suitable mineral materials to use in construction of the massive shield of a large low-background counting facility. These investigations prompted the development of techniques that have general application to environmental radiation studies and to certain geophysical problems. We have also collected a considerable body of data, bearing on both the environmental gamma-ray intensity and the concentrations of several gamma-emitters in a variety of rock formations.

We first discuss theoretical considerations, then describe our techniques for both field work and laboratory analysis. Finally, to illustrate applications of these techniques, we present some data organized to conform to the context of this meeting.

I. THEORETICAL CONSIDERATIONS; RADIOACTIVE ELEMENTS

Natural radioactivity in the earth's crust varies markedly with rock types. The principal radioactive elements that contribute to the radiation emanating from rocks are potassium-40, the uranium series, and the thorium series. These three elements all have very long half-lives, greater than 10^9 years, and all three emit gamma-rays as they undergo radioactive decay.

A. Potassium

Potassium is present in almost all of the earth's crustal material, and its isotope of mass 40 (K^{40}), is radioactive. The radio-isotope K^{40} comprises 0.0119% of natural potassium, and the ratio of K^{40} to K^{39}, 1/8500, is considered to be fairly constant throughout the earth's crust. The isotope K^{40}, with a 1.3×10^9 year half-life, has a branched decay scheme: about 89% goes to Ca^{40} with emission of a 1.3 MeV β particle; about 11% goes to A^{40} via electron capture and emission of a 1.46 MeV gamma-ray.

The principal potassium-bearing minerals are the feldspar orthoclase, the micas muscovite, and biotite. Hornblende and plagioclase may contain up to 1% potassium. The clay mineral, illite, also has potassium as a principal constituent. Though not a principal constituent of the clay mineral, montmorillonite, potassium may be incorporated by cation exchange with aluminum.

† This report is the prepared text of a contribution to the International Symposium on Natural Radiation Environment, presented by the authors at Rice University, Houston Texas on April 12, 1963.

In igneous rocks, the concentration of potassium varies roughly with the abundance of silica, potassium being more prevalent in the acidic igneous rocks such as granite than in the ultramafics (periodotite, dunite, and serpentine). Rankama and Sahama (1950) show that because of the large ionic radius of potassium (1.33A) and its twelve-fold coordination with respect to oxygen, the element is excluded from the early-formed crystallates of magmatic differentiation and becomes enriched in residual melts and solutions. Potash feldspars are therefore characteristic of the late crystallates, the igneous rocks most abundant in silica.

Ahrens (1954) gives the following concentrations of potassium for various igneous-rock types:

In granite, the range is from 2 to 6%.

In basalts, potassium concentrations vary with individual flows (potassium being sensitive to fractionation in a basaltic magma). A variation between 0.65 and 1.4% was found by Ahrens et al. (1952) in Columbia River Basalt. Daly (1933) measured 0.37% in oceanic basalt and 0.65% in plateau basalt.

Periodotite, pyroxenite, and dunite and their serpentinized forms have the lowest potassium concentrations of the igneous rocks--about 10 ppm.

The potassium content of sedimentary rocks depends largely upon the relative amounts of the feldspars, micas, and clay minerals that partially comprise the mineral-aggregate sediments. A sandstone derived from a close granitic source would contain an appreciable amount of feldspar and therefore exhibit a potassium content roughly that of its source granite. A pure quartz sandstone derived from a quartzitic source, or a sandstone at a great enough distance from its granitic source so that the feldspars have been removed during the transport, would contain a relatively low potassium concentration.

Shales or argillaceous sediments with an abundance of mica and clay minerals contain appreciable potassium. Limestones are generally low in alkalies, though the presence of the authigenic feldspars and some argillaceous material filling cracks in the limestone (hydromica developing from detrital clays during diagenesis of the limestone) may increase the percentage of potassium over that of pure limestone. Average potassium contents of the broad groups of sedimentary rocks (Ahrens, 1954) are:

Shales and argillaceous sediments	3%
Sandstones	1%+
Limestones	tenths of 1%

B. Uranium and Thorium

Uranium-238 (half-life 4.49×10^9 y) and thorium-232 (half-life 1.39×10^{10} y) and their decay products are also major contributors of radioactivity in the earth's crust.

1. Uranium and Thorium in Igneous Rocks

As with potassium, the uranium and thorium contents in igneous rocks vary with the percentage of silica. Along with being potassium-rich, the granites are usually uranium- and thorium-rich, while the ultramafics are

quite lean in all three elements. Keevil (1944) gives the probable value for the thorium-uranium ratio in igneous rock as 3.0 to 3.5. Evans and Williams (1935) show an almost linear relationship of K_2O with uranium concentration in the volcanic rocks of the Lassen Peak region. Adams (1954) attributes the nearly linear relationship to systematic concentration of both uranium and potassium in the liquid phase of the magma as crystal fractionation proceeded. Thus, uranium and potassium oxide were excluded to a degree from the common minerals formed during crystallization of the Lassen magmas. Uranium and potassium oxide do not substitute readily for other common ions because of the different space requirements of potassium and uranium. Their ionic radii and coordination numbers with respect to oxygen do not permit their ready substitution with other common ions. This would suffice as a partial explanation of the higher uranium and potassium concentrations in the more acidic igneous rocks.

Larsen et al. (1956) show from their study of the uranium concentrations of three Mesozoic batholiths of the western United States that, where fractional crystallization is assumed to have been the major factor in magmatic differentiation, uranium is enriched in the youngest rocks (those being high in SiO_2 and K_2O and low in CaO and MgO). A maximum enrichment of greater than 20 ppm is found in differentiates very poor in CaO. From chemical analyses of samples from the Southern California batholith, Larsen et al. show that the uranium content of the common rock-forming minerals increases with total uranium in the bulk rock as the percentage of silica increases in the rock.

Davis and Hess (1949) have studied the concentration of radium in ultramafic rocks. Average values for igneous rocks range from 0.01×10^{-12} g per g of radium in ultramafics to 1.0×10^{-12} g per g in felsic rocks. The absence of uranium (parent element for the radium) in ultramafics is attributed to its strong concentration in residual liquids during magmatic differentiation, with uranium being apparently excluded from the crystal structures of the early-formed minerals, olivine, pyroxene, spinel, and plagioclase. Uranium is four-valent at high temperatures with an ionic radius of 0.97 Å. This size may permit U^{+4} replacement of Ca^{+2} or Na^{+1}, but an eight-fold coordination is required with oxygen atoms. No such positions are available in the crystal structures of these early-formed minerals.

By comparing the concentration of radium in ultramafic rock samples with the percent weight loss of the samples at 1000°C (representing essentially the percentage of water present in the original rock), Davis and Hess (1949) show that the parent uranium was likely contained in the interstitial liquid trapped between accumulated crystals in the cooling magma.

In examining the distribution of radium in individual minerals comprising a sample of dunite, Davis and Hess found that tremolite--1.2% of the total sample composition--contributed 20% of the total radium; serpentine, talc, and kammererite--4.8% of the total sample composition-contributed 30%, while olivine--92% of the total composition--contributed 45%.

2. Uranium and Thorium in Sediments

Koczy (1954) states that even though uranium is highly insoluble, the uranyl ion is able to form complex compounds which are generally soluble. Thorium is also highly insoluble but does not form soluble compounds.

Therefore, uranium can be carried in an oxidizing environment, while thorium isotopes cannot. In river water, U^{238} is transportable in both solution and suspension, while Th^{232} is chiefly contained in mineral resistates and is hardly transportable in the dissolved condition because of its tendency to hydrolyze. Traces of uranium are also present in resistates. Therefore, because of the general insolubility of resistates in sea water, thorium and some uranium are deposited as heavy elements, usually near the coast or in river-mouth sediments. When compounds containing the uranyl ion reach a reducing (sapropelic) environment, uranyl complexes become reduced, and uranium is precipitated or absorbed as a four-valent ion. Areas such as the Black Sea and Norweigian fjords are examples of present-day sapropelic areas. A concentration of 50 to 100 ppm uranium is reported in late Quarternary sediments from Norwegian fjords. The concentration of uranium in sea water reaches a maximum at a depth of about 1000 m because of the reducing environment present at this level.

Petterson (1954) attributes the deficiency of Ra^{226} in sea water (there should be about 5×10^{-16} g of radium per 1 ml of sea water, but only about one-sixth of that is present) to the precipitation of the uranium daughter product, Th^{230}, from sea water along with ferric hydroxide. Therefore, a potential source of Ra^{226} is carried down to the surface of the sea floor. In the sea floor sediments, the fall-off of the radium content with depth in the sediments is irregular. There are two sharp maxima between 9 and 0-20 cm and very low radium values from 40 to 80 cm. Petterson proposes that radium migrates from its mother substance, Th^{230}, so that radioactive equilibrium between the two elements is not maintained.

Bell (1954) states that the separation of uranium from aqueous solutions can take place in reducing environments in the presence of carbonaceous material and sulfides and in the absence of dissolved oxygen. Uranium is adsorbed by clays, carbon, aluminum, manganese, and silica, and is accumulated with phosphatic marine sediments. The precipitation or adsorption of uranium is inhibited by the presence of the carbonate ion, which accounts for the generally low uranium concentration in limestones and dolomites.

The highest syngenetic concentrations of uranium occur in sapropelic marine shales. Large amounts of organic material and sulfides and a scarcity of carbonate are characteristic of these shales. All known uraniferous black shales are of pre-Mesozoic age. As opposed to the sapropelic sediments, the humic sediments (peats, lignites, and coals), which are characterized by low hydrogen and high carbon and oxygen contents, are generally low in uranium content. The presence of uranium in some Tertiary and Cretaceous lignites is attributed by some geologists to epigenetic deposition in the lignites, and by others to syngenetic deposition of uranium with the carbonaceous material

The occasionally appreciable uranium contents of colloidal sediments such as chert (formed as gelatinous or colloidal precipitates) may be due to the adsorption of the uranyl ion onto the silica-gel surface.

3. Uranium and Thorium in Accessory Minerals

Accessory minerals--primarily zircon and to some extent apatite, cassiterite, sphene, and rutile--carry appreciable but various amounts of

uranium and thorium. The phosphate, monazite, is the principal thorium ore-mineral. Frondel (1956) gives the average concentration of thorite ($ThSiO_4$) as 10 to 12% in monazite and up to 1% in zircon.

Larsen et al. (1956) state that the igneous accessory minerals--zircon, sphene, and apatite--have uranium concentrations of over 300 ppm. The uranium concentration of zircon increases with the radioactivity of the host rock from gabbro to granite.

Rankama (1954) attributes pleochroic discoloration in such minerals as biotite, chlorite, amphiboles, andalusite, and quartz to the effect on crystal structures of alpha and beta radiation from uranium and thorium. Pleochroic halos around minerals are most numerous in silicic igneous rocks and are practically nonexistent in the ultramafic igneous rocks. Radioactive minerals such as zircon, rutile, cassiterite, and apatite normally comprise the nuclei of the halos. The halos are usually made up of rings with characteristic radii. A ring in biotite due to U^{238} alpha emission has a radius of 12.7μ, while a ring due to Th^{232} in biotite has a 12.4-μ radius. Measurements of ring radii can thus be used to determine the range of alpha-particle penetration in crystals as well as the alpha particles' energy.

The effect of alpha emission on some minerals, notably zircon, results in production of nearly complete isotropy. The mineral appears in the amorphous state and is said to be metamictized. All zircons show some degree of radiation damage, and the primary cause of this metamictization is the presence of uranium and thorium in the mineral structure.

As well as being sources of radioactivity in igneous rocks, accessory minerals such as zircon, sphene, rutile, etc. have an appreciable effect on the radioactivity of sedimentary rocks. These minerals have a high specific gravity (about 3.5) so that they are concentrated with metallic minerals during deposition. When the radioactivity of zones of heavy-mineral deposition in the Ione formation is correlated with their mineralogy (T. C. Slater, private communication) there is evidence that the zones of highest radioactive background correspond to the areas of heavy-mineral deposition.

II. FIELD PROCEDURES

Our field operations normally involve a threefold procedure: determination of the geologic setting of the rock or soil exposure under study, radiometric scanning with a portable scintillation counter (described in detail in Part II-B), and sampling. A previous perusal of reports and geologic maps of the area studied aids us in the evaluation of the geologic setting of a site. Observations are made of nearby sources of contamination; e. g., higher radioactivity material which may influence the field counting rate of the soil or rock (see Part II-C).

A. Sampling

Sampling procedures vary depending upon the nature of the material under study. On bedded or laminated outcrops, pick-sample lines are cut perpendicular to the layered orientation. Homogeneous outcrops are chip sampled with an attempt made to obtain fresh material with as little fallout contamination as possible. Nearby outcrops of rocks with possibly different radiometric characteristics in the vicinity of a sampling site are also sampled to aid in the determination of their influences on the site's field counting rate. Rock samples are generally contained and transported in half-gallon cardboard ice-cream cartons.

Our work in soils has mainly been in conjunction with evaluations of the fallout component of radioactivity. Therefore, most of our soil samples are surface samples and incorporate varying amounts of vegetation. Soil sampling consists of taking the top 1 to 1.5 in. of an area roughly 2×2 ft. In some areas where we wish to determine the depth pentration of fallout we have also sampled the barren soil directly beneath the grass-root zone. Soil samples are generally contained in polyethylene "poultry bags" with the opening tied off to ensure little, if any, moisture loss. Due to their light weight and small space consumption we sometimes use heavy duty polyethylene bags for rock samples as well as for soil.

Our general field-sampling philosophy is to get the most representative sample of a rock outcrop or soil site from a minimum amount of material; therefore the sampling method varies somewhat from site to site.

B. Portable Instrument

The radiation detection instrument used for this field work was designed and built at the Lawrence Radiation Laboratory; details of the circuitry have been published by Goldsworthy (1960). A brief description of the instrument is included here, followed by a general outline of the way it was used in this project.

The detector is a 3-in. -diam by 3-in. -thick thallium-activated sodium iodide [NaI(Tl)] scintillation crystal, viewed by a Dumont 6363 3-in. -diam photomultiplier tube. The detector assembly is housed in a 5-in. diam by 12-in. -high thin-walled stainless steel case, and is connected to the indicator unit by 5 ft of coaxial cable. The indicator unit contains a Cockroft-Walton-type high-voltage supply for the phototube, a four-transistor linear pulse amplifier, an integral pulse-height selector circuit, and a multirange count-rate sensitive indicator circuit. All electrical power for the instrument is

supplied by a single self-contained 10.75-V mercury battery. A fresh battery can be expected to provide at least 300 hours of instrument operation time. The relatively large NaI(Tl) crystal provides a count rate high enough that we can always achieve a steady and reproducible reading from the count-rate meter; thus we do not have to resort to earphones, even when assaying the lowest intensities.

Four linear ranges are used in the count-rate circuitry to span the wide latitude of radiation intensity encountered. The ranges are calibrated to span intervals of 0 to 100, 0 to 500, 0 to 5000, and 0 to 50000 counts/sec, by the use of a single meter scale marked with 50 equal divisions. These calibrations are established by use of a variable-frequency pulse generator to determine correct adjustment of circuit values; both full-scale deflection and scale linearity are thereby checked.

After the electronic calibration is satisfactory, we calibrate the instrument in terms of radiation intensity. The detector unit is first connected to the 100-channel pulse-height analyzer, and we record the gamma-ray spectrum produced by room background. Our original examination of this spectral shape, along with several other considerations, showed that the instrument threshold should lie above the 100-keV gamma-ray energy; we chose a value of approximately 120 keV. After the background count rate has been determined from pulse-height-analyzer data, the detector is reconnected to the indicator unit, and the threshold control is adjusted until the meter indicates the correct count rate. Of course, these two operations are performed in quick succession, while measuring the same background intensity.

We then expose the detector to known intensities of gamma rays from Ra^{226} sources certified by the National Bureau of Standards. Using count rates observed from these precisely known radiation intensities (corrected for background) we can establish calibrated ranges in terms of Ra^{226} (in equilibrium with its decay products).

This calibration procedure is performed infrequently, usually when there is evidence of erroneous instrument behavior. We employ a simple method for routine calibration checks; a disc source of refined uranium is used here. The correct count rate must be observed from this source when it is in a standard position (against the detector case end-plate nearest the crystal), if instrument readings are to be considered valid. The gamma-ray spectrum from this check-source has a steep slope at the energy corresponding to the instrument threshold; thus, the test provides a sensitive means to verify correct instrument performance.

The Ra^{226} gamma-ray calibrations of the four ranges are listed in Table I. The most frequently used scale is the 0 to 0.0125 mr/hr range; each scale division corresponds to 0.00025 mr/hr. The most sensitive scale, used for lowest intensity measurements, provides scale divisions corresponding to increments of 0.00005 mr/hr, or 0.05 μr/hr.

Data taken with the 100-channel pulse-height analyzer show that, to a first approximation, normal mineral samples, unshielded natural background radiation, and Ra^{226} in equilibrium have spectra of the same gross shapes as viewed by our crystals. Thus the Ra^{226} calibration is very useful in practice, for it can be applied generally to convert field data into meaningful radiation-intensity values.

Table I. Ranges for the portable scintillation counter, and calibration with respect to Ra^{226}

Scale range (counts/sec)	Scale range (mr/hr)	Smallest scale division (mr/hr)
0 to 100	0 to 0.0025	0.00005
0 to 500	0 to 0.0125	0.00025
0 to 5000	0 to 0.125	0.0025
0 to 50000	0 to 1.25	0.025

For field use, calibration checks are normally made twice during a measurement sequence: just after turn-on, and just before turn-off of the instrument. One check may be sufficient for single-point measurements. For surveys lasting an hour or longer, the uranium source may be carried along by a second person so that frequent checks can be made (the main concern here is that damage to the instrument may result from vibration and shock inflicted while negotiating rough terrain).

C. Field Use of the Instrument

We now discuss field use of the instrument, particularly to clarify the significance of measurements taken in the field. The instrument is usually carried with the detector about 2 ft above ground level. Response time of the count-rate circuits is rapid enough so that significant changes in radiation intensity are registered while the surveyor walks at a normal pace. Lowering the detector to the surface will permit a more precise assay of the radioactive content in the volume immediately beneath.

Some survey work has been attempted with the detector carried inside a moving vehicle. We soon learned that the only quantity to be measured with confidence by this technique is the radioactive content of the roadbed; such information is generally of secondary importance. Information obtained while traversing narrow gravel or dirt roads may be the exception; these roads are usually of much more "local" character than wide, paved highways. However, when unequivocally correct data are to be obtained, there is no substitute for literally getting into the field. Some improvement in quality of mobile data would be realized if the detector were positioned 10 to 15 ft above the surface; this approach has been used by British workers as a surveillance technique in areas adjacent to reactor sites(Cavell and Peabody, 1961).

Problems of interpretation arise when surveys are taken in the vicinity of, or across, areas of sharply contrasting radioactive content. When moving from an area of high activity into an area of low activity, readings will not decrease exactly in accordance with the changes in rock activity. For example, a survey taken from Franciscan sandstone across a sharp surface contact into serpentinized rocks will indicate a rather abrupt decrease in intensity just as the contact is passed, but will also show an additional gradual decrease

as one moves further into the ultramafic formation. An apparent activity decrease may be noted for several tens of feet into the serpentine. In reality, laboratory analysis may show that the entire activity change occurs across a distance measured in inches, or fractions of an inch. The contribution of undesirable radiation in this situation can be reduced substantially if the detector is lowered to the surface. Additional protection from the high intensity area can be provided by digging a shallow pit for the detector, or by piling loose material around the detector to form a low barrier. Care must be exercised that such barriers are built of the same material as the formation to be assayed.

When the detector views a large area of uniform radioactive content, the measured intensity will remain nearly constant if the detector is lowered to the surface. Conversely, when the intensity changes, say, 10% or more for this test, the measured intensity is probably not characteristic of the bulk formation at hand. Float from a nearby area may influence the reading; so may sloughing overburden or a variety of other geologic conditions. In short, one must always study the local geologic and topographic features carefully to ensure that radiation-intensity measurements are interpreted correctly.

We have encountered a surprisingly wide latitide of radiation intensity in our survey of various rock formations. For example, the highest intensity from surface material (not considered to be of radioactive-ore grade) was a reading of 1400 counts/sec observed over latite from the Table Mountain flows west of Jamestown, California. Readings across a sharp contact between Table Mountain latite and serpentine ranged from 1400 counts/sec over the latite to 160 counts/sec over the serpentine. Here is a good example of the problems that arise in interpretation of field measurements; the serpentine is virtually free of radioactivity.

The lowest-intensity surface readings were 20 to 30 counts/sec, observed in serpentine at several localities. Some of these serpentine deposits are located within 2 to 3 miles of the Table Mountain formation. We note that lower readings are never observed at the surface, even over areas of freshly exposed serpentine--material that laboratory analysis shows to have essentially no measurable radioactive content. Thus, we attribute a significant fraction of the 20 to 30 counts/sec reading to airborne activity and to cosmic rays. The lowest intensity we observed was in a magnesite mine where serpentine is the host rock. A reading of 2 counts/sec was noted at a position 1200 ft in from the portal and under about 300 ft of cover. We hope to be able to obtain gamma spectra at this location in the future. Laboratory experience shows that most of the residual count rate derives from radioactive content of the detector assembly itself. It is interesting to note that our detector reads 6 to 8 counts/sec inside a "standard steel room" low-background facility at the Donner Laboratory, Lawrence Radiation Laboratory, Berkeley.

Some field scanning, primarily at limestone formations, was done in conjunction with a Precision Model 111 B scintillation counter. It was observed that readings were not as steady or reproducible on the Precision instrument as on the Lawrence Radiation Laboratory counter. However, the Precision instrument had sufficient sensitivity to detect contrasts between the carbonate rocks and surrounding higher-background materials. The Precision instrument uses a considerably smaller scintillation crystal than is used in the

Lawrence Laboratory counter, and therefore must operate with a much lower count rate; this factor alone can account for the different characteristics just mentioned. It can be assumed that a high-quality commercial portable scintillation counter that uses a crystal of size comparable to ours and is capable of registering radiation intensities as low as 0.0005 mr/hr can be successfully utilized for low-background gamma-ray surveys.

D. Field Spectrometry

We have just begun to study the application of gamma-ray spectrometry to field work. Figure 1 shows a spectrum taken over soil at a location outside our laboratory building in March 1963. Two important points are noted here. First, a very strong fallout peak is noted in the low 30's channel group. Second, the great intensity of low-energy air and ground scattered gamma-rays masks spectral structure below ≈ 0.6 MeV. The upper spectrum on this figure was taken with the detector in its normal housing, as might be used in field work. The lower spectrum was taken at the same site, but with a 1/8-in.-thick Pb absorber surrounding the detector assembly. The spectra are normalized to coincide beyond ≈ 1 MeV energy. Absorption data for 1/8-in. Pb thickness shows that 0.5 MeV gamma rays suffer attenuation by a factor of two, that the lower energies are more strongly affected, and that higher energies are less strongly affected. Thus, a thin Pb absorber should produce clarification in the spectral region above ≈ 0.3 MeV without too great a sacrifice in count rate caused by attenuation. In particular, the strong 0.61 MeV gamma ray from the uranium decay series should stand out clearly, when it is not overwhelmed by fallout peaks. In our example, the Zr-Nb peak does just such a masking job; however, this soil is not very rich in uranium. We intend to make two points by this example: that fallout is now a serious problem for surface spectral measurements, and that a thin Pb absorber, surrounding the detector, can add considerable clarity to field spectra. Absorber use may therefore aid significantly in identification of the isotopes present, particularly in the case of uranium, where other spectral areas are not so favorable for these purposes.

In the field, one expects a situation in many ways similar to that obtained in the laboratory by Gregory and Horwood (1961): nearly all observed gamma rays originate from the top 1-ft layer of ordinary earth material. In addition, there is present a very strong, low-energy air-scattered component that obscures structure at the low end of the spectrum. Use of thin 1/16 to 1/8-in. thick Pb absorbers may be very advantageous here, although such absorbers are not important for the simple count-rate scanning we normally perform.

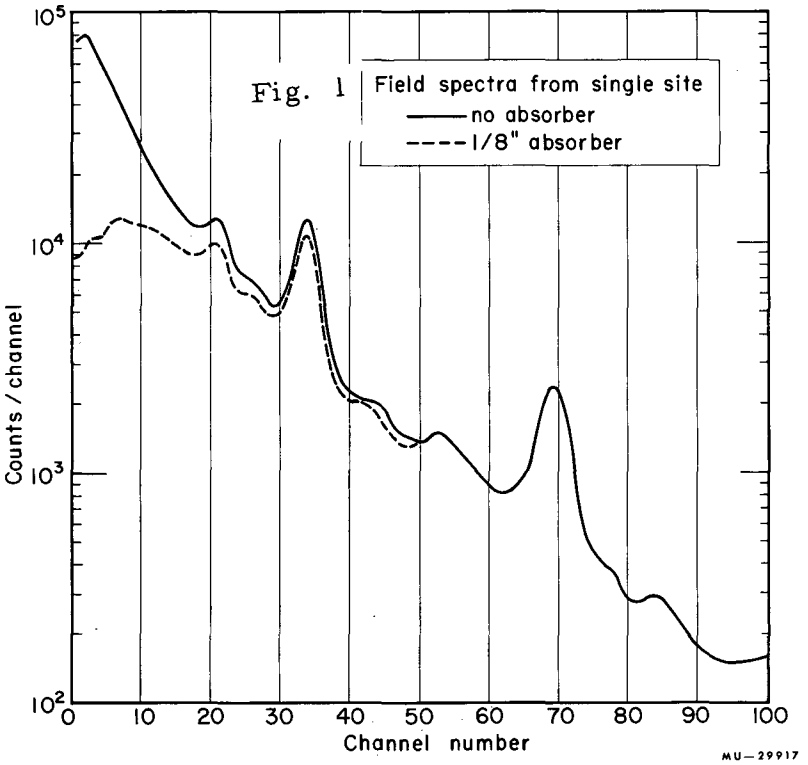
Fig. 1
Field spectra from single site
no absorber
1/8" absorber
Counts / channel
Channel number
MU-29917

III. LABORATORY PROCEDURES

In the laboratory a gamma-ray spectrographic analysis was conducted on each sample collected in the field. Usually one or more petrographic thin sections were prepared on representative samples from the field collection process. A description of the spectrographic equipment, evaluation and calculation procedures, and representative gamma-ray spectra are included in the following sections.

A. Preparation of Samples

Samples are prepared for gamma-ray evaluation by a standard procedure. Materials having pieces greater than 1 to 1.5-in. diam are reduced in size by hand crushing to 1-in. diam or smaller; materials already within this size range are used as received. Each sample is handpacked in a thin-walled polyethylene container measuring 4-in. diam by 3.5-in. long. We use commercially obtainable Tupper refrigerator food containers. The weight of contained material ranges from 500 to 1500 g; typical samples prepared from materials with bulk specific gravities of 2.5 to 3.0 weight 700 to 1000 g.

Great care is taken to ensure that sample materials do not become contaminated with foreign radioactivity in any phase of the work. Samples are placed in closed containers immediately upon collection, and are removed from these containers only when they are to be prepared for gamma-ray analysis. Sample preparation, handling, and storage are carefully controlled in this respect. All samples thus far analyzed have been retained, so that we can re-examine specimens as required.

B. Equipment

We use a gamma-ray scintillation spectrometer in the laboratory to assay the radioactive content of sample materials. The detector unit consists of a 4-in. diam by 2-in. thick NaI (Tl) scintillation crystal coupled optically to a Dumont-type 6363 phototube; the unit is constructed of special low-radioactivity materials. The detector and a sample to be counted occupy one compartment inside a lead shield. Interior dimensions of the detector compartment are 6-by 8-by 24 in. The shield itself is built of standard 2- by 4- by 8-in. lead bricks, and presents at least a 4-in. thickness of lead to all external radiation sources. A second identical shield compartment houses an identical detector, which is used exclusively to measure background radiation during each sample run. The background detector is shielded from the sample detector by a 4-in. thickness of lead. Both compartments are actually part of a single shield structure. The entire lead shield is covered with 0.030-in. cadmium sheet which is in turn surrounded by an 8-in. thickness of low-activity concrete blocks; both these materials serve as neutron-absorbing elements.

A separate background detector is used because the background (BKG) inside the shield is not constant. We need to measure sample activity that produces a net count rate that is only 1% of the background count rate; therefore our knowledge of the background must be exact. The only reasonable way the BKG variation can be followed with sufficient precision is to use a second detector (identical to the sample detector) for background determination

during each sample run. Problems related to background determination are fully discussed in Sec. III-E.

Output signals from each scintillation crystal are sent to identical UCRL Model-6 linear pulse amplifiers. Amplifiers are operated in the double-delay-line clipping mode in order to minimize problems created when very large overload pulses must be handled (cosmic-ray mesons traversing crystals of this size may deposit 70 to 80 MeV energy).

Information from the sample detector drives a Penco PA-4 100-channel differential pulse-height analyzer (PHA). The gain of the system is adjusted so that each of the 100 equal-width channels is 20-keV wide, and the total gamma-ray energy interval spanned is 0.080 to 2.08 MeV. The pulse-height analyzer accepts amplitudes in the 4- to 104-V range from amplifier output pulses up to an amplitude of 150 V.

Sample data are also recorded on four integral scalers, as follows:

(a) total counts in PHA channels 1 through 100.

(b) total counts above PHA channel 100.

(c) total counts above PHA channel 10 (0.28 MeV).

(d) total counts above PHA channel 80 (1.68 MeV).

The background detector system is adjusted to have exactly the same gain as the sample system, and the resultant information is recorded on three integral scalers, as follows:

(a) total counts above PHA channel 10 (0.28 MeV), on two units in parallel, to verify the data; this is the background correction number.

(b) total counts above PHA channel 80 (1.68 MeV).

We count the fast-neutron flux on an eighth scaler, utilizing a moderated BF_3 counter as the detector.

At the completion of a run, stored PHA data are tabulated on a Victor Printer adding machine and are simultaneously plotted in a semilogarithmic mode to produce a curve of the counts per channel vs energy (Figs. 3 through 9 are examples of curves derived from several runs.)

The initial calibrations of energy vs channel number for both systems and the PHA were performed with sources of known, different, gamma-ray energies. Routine calibration, performed at least once a week, includes:

(a) Centering the peak from Cs^{137} exactly in channel 29 for both crystals.

(b) Adjustment of all integral scaler thresholds, using precision pulse generator and the PHA to determine accurately the correct pulse amplitude for each threshold.

Most sample spectra show pronounced peaks from the included radioisotopes; the K^{40} peak is particularly useful in this manner, and proper energy calibration of the sample crystal can usually be confirmed by inspection of plotted data. Amplifier output signals are always displayed on an oscilloscope, to assist early detection of electronic troubles and thereby minimize collection of worthless data.

A Stabiline line-voltage regulator provides all ac power for this equipment. All dc power is derived from separately regulated supplies. The equipment is located in a fully air-conditioned laboratory and operates continuously except as required by servicing. Thus we have taken all reasonable steps to ensure stable operation of equipment and acquisition of the greatest amount of valid data.

C. Counting Procedure

Prepared samples are always counted with the container lid against the flat face of the detector crystal case; thus, the counting geometry is constant. Sample counting time depends upon the amount of radioactivity present and the precision required for the data. Lower radioactive content requires longer count time for any specified accuracy; conversely, greater accuracy demands longer count time for any given radioactive content.

The most active samples, which produce count rates 2 to 10 times the background rate in our selected energy band, can be analyzed in 50- to 150-min runs. Samples with intermediate activity can be analyzed in 200- to 500-min runs. The lowest-activity samples are counted for 600 to 2000 min; even the longest runs do not always provide the precision we desire, but must be terminated because of practical time limitations and restrictions of present detection sensitivity.

D. Sample Thickness and Spectrometer Response

We cast a series of 4-in. diam discs from a high-activity, uranium-rich cement. These discs, of measured thicknesses, were then used to explore the response of our spectrometer crystal to various thicknesses of samples. Figure 2 shows some results of these tests, and indicates clearly that little is to be gained in our system by increasing sample thickness beyond the dimension now in use. The limitation here mainly results from a decrease in the solid angle subtended by the more distant sample layers, rather than resulting from gamma-ray absorption within the intervening sample material. The use of a larger diameter crystal, or location of the entire sample at greater distance from the crystal, would show that layers at greater depth within a sample will still contribute a significant count rate increment. Gregory and Horwood (1961) found that their crystal-sample relationship required at least a foot thickness of crushed material before the addition of more material gave no significant count-rate increase. In short, each different crystal-sample configuration will show a unique relationship between observed count rate and sample thickness. Thus, calibrations must be performed for each configuration if quantitative results are to be obtained. Because calibration procedures are relatively difficult, we have settled upon one configuration for all laboratory work; this configuration, at the same time, provides the highest detection efficiency from a simple sample-container shape.

Our spectra show distinct sharp peaks for all prominent gamma-rays down to and including the 0.24 MeV member of the thorium series. This is a definite aid to identification of the radioactive components present. Gregory and Horwood (1961) also show that increasing sample thickness gradually obscures peaks at energies below 1 MeV, until at the 1-ft depth, these peaks may be little more than shoulders along the spectrum. Good spectral resolution

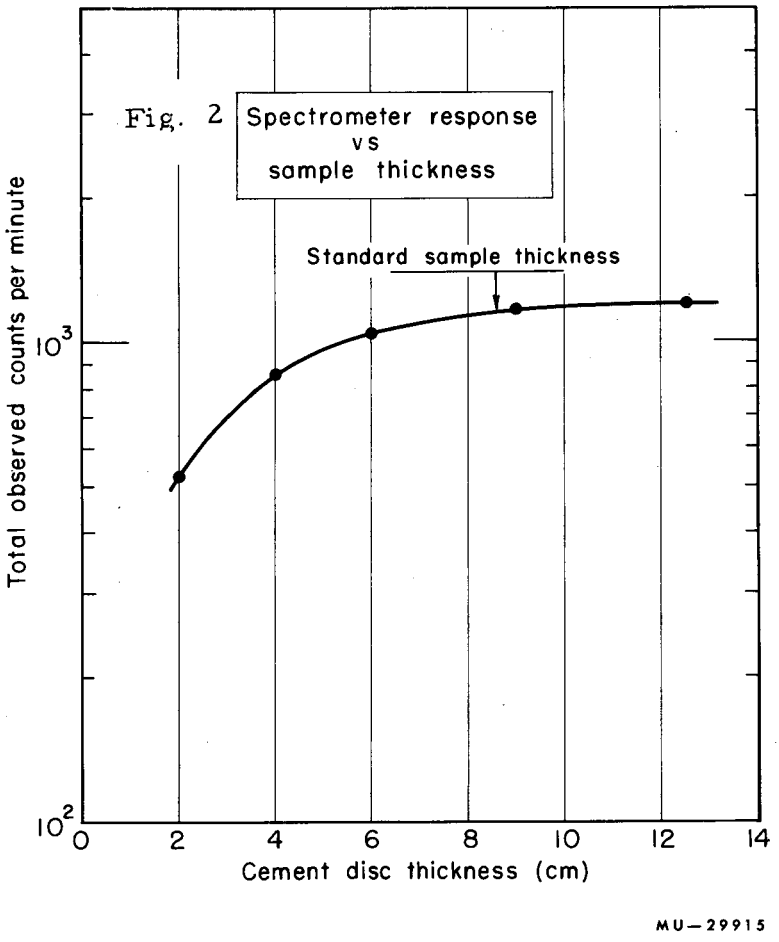
Fig. 2 Spectrometer response vs sample thickness
Standard sample thickness
Total observed counts per minute
10^3
10^2
0
2
4
6
8
10
12
14
Cement disc thickness (cm)
MU-29915

and maximum count rate are seen to be incompatible, and each worker must make a compromise here.

E. Background Count-Rate Considerations

The data from a sample run include both sample and background information. We infer the correct background to subtract from the sample count rate by use of data from the second detector and a set of background correction tables. These tables were derived from a number of long (about 1000-min) runs in which both detectors measured background. Background data for all energy intervals of interest were fitted by the least-squares method to linear equations, which were then used to generate tables that relate background detector data to sample detector background. By this technique, we can infer the correct background to within ±1 count/min, while the quantity we infer varies from 220 to 270 counts/min.

The background variation is found to be related linearly to the slow-neutron flux at the detector. This variable neutron flux is produced by high-energy particle accelerators located about 1/3 mile from our detectors. The background count rate observed in the lead shield showed variation greater than a factor of 2; this was an unacceptable situation. We first covered the entire shield with a thin cadmium layer, to reduce the slow neutron effect. Even so, the background increased from 220 to 270 counts/min when the external slow-neutron flux increased from 0.005 n/cm^2-sec [cosmic ray intensity near sea level, Patterson, et al. (1959)] to 0.030 n/cm^2-sec (typical accelerator-produced intensity at our site). We then added an outer layer of low-activity concrete blocks to provide moderation and absorption of fast neutrons. The background variation has thereby been reduced so that the range lies between 220 and 230 counts/min for various accelerator-operating conditions. The changes are now related to the external fast neutron flux, although they do not follow so regularly as before addition of the concrete. The relationship between backgrounds in the two crystals does still follow as closely, though.

Other experiments with these crystals in the same close-fitting lead shield show that neutron-produced background effects are caused primarily by slow-neutron capture, either as a prompt capture radiation, or as decay radiation from induced activation. By far the most important item for both these processes is the crystal itself. We have determined that the 25-min half-life isotope I^{128} is the most serious activity induced, and that activation to equilibrium in a thermal neutron flux of 1 n/cm^2-sec produces an observed decay count rate of ≈1700 counts/min immediately following such an irradiation. Under equilibrium conditions during an irradiation in unit thermal flux the total observed count rate is ≈6200 counts/min. The implications of these facts to accurate low-level counting situations are obvious.

Figure 3 illustrates the sort of spectrum observed in a long background run with the sample crystal. The shape is rather undramatic; the only definite features are provided by backscatter effects in the low channels, a weak annihilation radiation peak at channels 21 to 22, and a modest K^{40} full-energy peak centered around channels 68 to 70. The backscatter effects derive principally from the small interior dimensions of our shield; the annihilation-radiation peak is associated with both cosmic rays and neutrons;

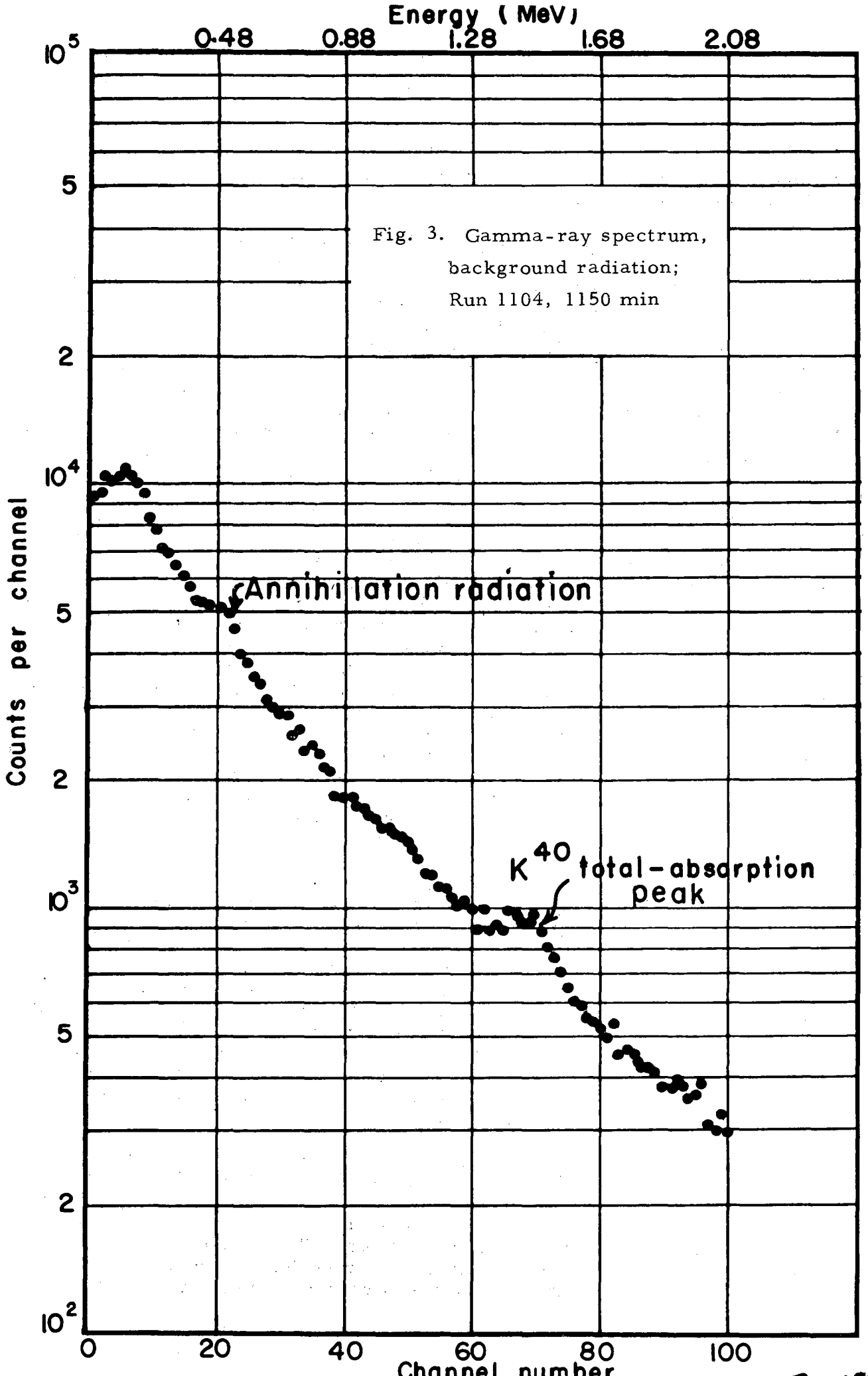

Fig. 3. Gamma-ray spectrum, background radiation; Run 1104, 1150 min

the K^{40} peak is produced by potassium in the glass phototube envelope. Other minor contaminants are probably masked by these predominant activities.

It is worth noting that when a reasonably low background is obtained, successful measurement of small increments to this background depends more on constancy than on magnitude. Our concern for accurate background data is thus understandable.

F. Data Analysis

Data obtained from sample materials are analyzed with varying degrees of sophistication. We describe the analysis steps here, and indicate the kinds of information derived from treatment of data by such methods. We will assume that data have been corrected for background, if no mention of this correction appears in the text.

The simplest analysis involves use of only the total stored counts: a summation of channels 1 through 100. These data are reduced to values of specific activity for each sample, expressed as counts/min-g. The single number so obtained is a measure of the total gamma-ray activity of the sample detected by our crystal; however, we learn nothing about the identity of the radioactive isotopes from this simple analysis.

A second simple analysis technique involves inspection of the 100-channel differential spectrum, performed most effectively by use of the semi-logarithmic data plot acquired for each sample run. We compare such a sample plot with plots of standard spectra obtained from materials that contain only uranium, thorium, or potassium, singly (for a discussion of standard spectra, see Part III-G). The comparison shows which of these three is present in considerable abundance, and can indicate relative amounts of each substance in favorable cases.

We obtain quantitative information for the three normal radioactive components (uranium series, thorium series, potassium) from a detailed analysis of each 100-channel spectrum. The procedure involved and an example of its application are set forth in the following paragraphs.

The calibration spectra of the three components (U, Th, and K) were examined, and three energy groups chosen which exhibited dissimilar shapes in each spectrum when compared with the other two. Each interval contains a nonzero fraction from its respective complete spectrum. These nine numbers are used as the constants of a set of three simultaneous equations in three unknowns (U, Th, and K). Sample count rates from the same three intervals are inserted in the equations; solution of the equations then yields values for U, Th, and K in the sample. The values so obtained are in terms of count contribution from each component present in the entire spectrum. The sum of the calculated components is compared to the observed sample activity, to provide one check for validity of the process.

The three intervals selected are channels 41 through 50 (0.88 to 1.08 MeV) 51 through 60 (1.08 to 1.28 MeV), and 62 through 74 (1.30 to 1.56 MeV). The two lower intervals provide contrasting shapes in the U and Th spectra,

a condition required for obtaining unambiguous solutions from the equations. The highest interval includes the total absorption peak of K^{40}.

Several other considerations enter into selection of energy intervals for this analysis. The first factor is simply the necessity to acquire enough counts per interval to permit a meaningful solution of the equations with respect to statistical counting errors. We are thus encouraged to use low energy intervals, thereby taking advantage of greater crystal efficiency at low energies plus Compton contribution in these channels from higher-energy gamma rays. The second factor warns us to stay relatively high in energy to avoid backscatter problems and self-absorption within the sample of the low-energy gamma rays. A third factor is important for those samples that contain "old" fallout. The highest gamma-ray energy present in "old" fallout comes from Cs^{137}, at 0.661 MeV, and produces a peak centered in channel 29 that extends into the low 30's. The effects of recent or fresh fallout are discussed in detail in Sec. IV. The lowest interval for the U, Th, and K determination must lie above this peak, or erroneous results may be obtained. Furthermore, choice of the three intervals above the Cs^{137} peak permits us to calculate an approximate count contribution of "old" fallout to a spectrum. Thus we standardize the three intervals for all samples to make them compatible with fallout-bearing samples, rather than generate multiple sets of parameters for different classes of samples.

Early attempts to use two energy intervals above the K^{40}-peak position for U and Th determination met with little success; we could not acquire enough counts in these intervals in reasonable run times to provide acceptable precision for calculated activity values. The problem of low count rate also applies to use of the 2.62 MeV total-absorption peak for thorium determination, although a lower background and the presence of only the thorium component at this high energy do favor the use of this interval. A larger crystal would provide greater response at 2.62 MeV and therefore make this peak more useful for thorium assay. For the present, the 2.62 MeV peak region can serve as a check for thorium values computed from the three-interval method.

The set of equations from each sample run is solved by use of third-order determinants. Solutions are obtained by direct numerical computation or by use of a programmed digital computer. We first show derivation of the constants used in these equations, and then work a sample calculation to illustrate the procedure.

The constants are derived from three simultaneous equations:

$$C_1 = 1.0000\ U_1 + 1.0000\ Th_1 + 1.0000\ K_1 ,$$

$$C_2 = 1.3016\ U_1 + 0.9107\ Th_1 + 0.4261\ K_1 ,$$

and

$$C_3 = 1.3024\ U_1 + 3.6796\ Th_1 + 0.4389\ K_1 ,$$

where C_1, C_2, and C_3 are the total counts (after background is subtracted) in channels 62 through 74, 51 through 60, and 41 through 50, respectively; and U_1, Th_1, and K_1 are the count contributions in the C_1 interval. The coefficients in these equations were determined from spectrometer runs of the standard uranium, thorium, and potassium samples. The coefficients are normalized to values of unity in the C_1 interval for convenience.

Third-order determinants were used to solve the above equations in terms of U_1, Th_1, and K_1: we have

$$U_1 = (-0.4830)\, C_1 + (1.3398)\, C_2 + (-0.2004)\, C_3,$$

$$Th_1 = (-0.0067)\, C_1 + (-0.3570)\, C_2 + (0.3620)\, C_3,$$

and

$$K_1 = (1.4897)\, C_1 + (-0.9828)\, C_2 + (-0.1616)\, C_3,$$

where now U_1, Th_1, and K_1 are the contributions of uranium, thorium, and potassium to the C_1 interval, and C_1, C_2, and C_3 are the count contributions in each interval from a sample spectrum. These are the three equations used to compute the radioactive components of all samples. The U_1, Th_1, and K_1 values are then multiplied by 40.368, 69.593, and 5.2858, respectively, to calculate U_t, Th_t, and K_t, the contribution of each component to the total spectrum. These results can then be used with sample weight and carefully determined calibration factors to compute actual concentrations for U, Th, and K in each material. We illustrate by example.

Sample Calculations: "TOP SAND", Run 806, 1009 g weight, 140 min. run time

Channel group	62-74	51-60	41-50
Counts	4530	3207	4456
Counts/min	32.36	22.91	31.83
BKG*	10.50	10.31	14.73
Net counts/min	21.86 (C_1)	12.60 (C_2)	17.10 (C_3)

U_1 = 2.898; multiply by 40.368 = U_t = 117 counts/min

Th_1 = 1.544; multiply by 69.593 = Th_t = 107 counts/min

K_1 = 17.418; multiply by 5.2858 = K_t = 92 counts/min

Sum = 21.860 (C_1 check) — 316 counts/min calculated total (329 counts/min observed total)

Uranium assay at 127,970 counts/min-g of U: concentration = 0.91 ppm

Thorium assay at 51,526 counts/min-g of Th: concentration = 2.09 ppm

Potassium assay at 15.845 counts/min-g of K: concentration = 0.58%.

Such calculations are easily performed in a few minutes with a desk calculator; it is our general procedure to compute each run in this fashion, and to use the programmed digital computer for special situations.

*BKG data obtained from tables at BKG detector = 259 counts/min this run.

Treatment of statistical errors as they appear in calculated components is rather cumbersome if exact expressions are used. However, if we make several simplifying assumptions the errors can be computed rather easily to yield values that are approximately correct for most cases. These assumptions are:

(a) Errors in the nine parameters obtained from the U, Th, and K calibration spectra are very small.

(b) Errors in the nine coefficients calculated from the above parameters are small compared to errors of the C_1, C_2, C_3 quantities measured in sample runs; errors in these coefficients can therefore be neglected.

(c) Errors in C_1, C_2, and C_3 are nearly the same in magnitude and can therefore be considered equal.

When these three assumptions are applied to our analysis method, the approximate errors become

$$\sigma\ U \approx 57\ \sigma\ C_1\ ,$$

$$\sigma\ Th \approx 34\ \sigma\ C_1\ ,$$

and

$$\sigma\ K \approx 9.2\ \sigma\ C_1\ ,$$

where the errors are standard deviations of the computed values for U, Th, and K in the total spectrum, expressed in counts/min, in terms of the error in C_1. (Exact treatment of errors in our IBM 7090 Computer program confirms that these expressions are good approximations.) Note that the absolute magnitudes of these errors are not dependent upon the amounts of U, Th, and K; thus the relative errors (percent errors) in the three components are inversely proportional to their abundances. Consequently, it is difficult to measure accurately a small amount of one component in the presence of a large amount of another component.

The errors discussed here are only those due to the statistical nature of the counting procedure, and do not include such factors as inhomogeneity of activity distribution in samples, or differences in gamma-ray absorption within samples due to differences in atomic number and total weights. Such factors should be explored and their magnitudes determined, so that the technique can be improved to yield more precise information.

We have enlisted the aid of an IBM 7090 digital computer in an effort to extract the maximum information from our 100-channel spectra. Although this program is just now in the development stage, some early results are suitable for discussion here.

The first computer analyses are designed to check the validity of our method, to calculate statistical errors of results, and to separate the fallout component spectrum from any sample spectrum. Computer input data include 100-channel spectra from the U, Th, and K calibration samples, a standard background, and the sample runs to be analyzed, along with other pertinent sample run data. The computer first makes a background correction and then calculates U, Th, and K quantities, using the three-equation method. Errors are computed for these quantities from exact expressions. The U, Th, and K solution is next used to synthesize a 100-channel natural activity spectrum.

This natural activity spectrum is subtracted from the background-corrected observed spectrum to produce a third spectrum. This residual spectrum, which we call "fallout," shows the differences between an observed sample spectrum and its calculated natural-activity spectrum, and so includes statistical errors, any systematic errors, and the actual fallout spectrum. Computer readout includes solutions for U, Th, and K concentrations with errors, the background-corrected observed spectrum, the synthesized natural activity spectrum, and the "fallout" spectrum.

Two classes of samples have been examined in this fashion: those known to be free of fallout, and those known to contain fallout. A study of the results from fallout-free samples has not yet revealed any systematic errors in our assay methods. In the strictest sense, this just means that the sample materials produce spectra indistinguishable from linear combinations of the calibration spectra. No direct verification for our actual assays is obtained from this sort of analysis. The residual 100-channel spectra do not show regular shapes, such as would be the case if, for example, the calibration spectra were in error. One exception is noted, and that is found in analyses of the virtually nonradioactive ultramafic samples. Here we see a cluster of residual counts in the low energy channels that show a regular shape--just that shape which should appear from backscatter effects (see Sec. III-H).

Fallout-bearing samples produce residual spectra we have come to recognize as true fallout spectra. We have concentrated mainly on soil samples, from which we seek to determine the fallout contribution. The residual spectra are smooth, except where statistical errors are relatively large. We note one effect in a number of these spectra that may be a systematic error if it persists after a larger group of samples in analyzed. This effect appears as two artificially deep valleys in the fallout spectra, and results from an overestimate of the uranium content.

We are expanding the scope of computer analysis, to include a search for more favorable spectral intervals for U, Th, and K determinations: lower-energy intervals would certainly improve the accuracy of our assays. A careful study will be made to determine the improvement in accuracy obtainable by imposing some limit conditions from various portions of the spectrum on the allowable solutions for U, Th, and K. Other methods of solution will also be studied.

G. Standard Samples

The U, Th, and K contributions to the total gamma-ray spectrum from a sample are calculated by use of coefficients developed from standard spectra. These standard spectra are explained in detail here, so that a clear understanding of our methods can be obtained. We have acquired separate assayed samples of uranium ore and thorium ore that are certified to be in secular equilibrium with their respective decay series. It is very important that equilibrium exists in the calibration samples; otherwise, distortion of spectra will result, especially if late members of the series are lacking in abundance. This lack of equilibrium would also lead to incorrect assays for experimental samples.

The assayed equilibrium ores of both uranium and thorium were obtained from the U. S. Atomic Energy Commission's New Brunswick Laboratory, New Brunswick, New Jersey. We have prepared samples for calibration purposes, using the standard polyethylene containers and two different bulk dilution materials. In each case, known amounts of the assayed ores were carefully mixed with known amounts of bulk material, and then packed into the containers. The bulk materials used are (a) Jefferson Lake minus 50-mesh serpentine fines, and (b) Clemco No. 24 silica sand.

No significant differences in either the spectral shapes or count rates were noted when an ore was analyzed in these two matrix materials; however, since the particle sizes of ore and matrix are more nearly equal with serpentine fines than with sand, a better mixture is obtained using serpentine as the matrix. Discussion of the results of calibration runs is limited to those obtained with the ore-serpentine mixture.

The New Brunswick Laboratory (NBL) ores are in the form of nominal 100-g samples of accurately known concentrations of each ore diluted in and thoroughly mixed with finely ground dunite. The uranium ore used to make the calibration sample was the 0.50% uranium concentration member of the NBL-42 series. This uranium ore is certified to be in equilibrium by measurement of the radium to uranium ratio, and contains a negligible amount of thorium. A 50-g quantity of this ore was mixed with 850 g of serpentine fines and packed in a polyethylene container to constitute our uranium calibration standard. The thorium ore used was a 1.01% thorium concentration member of the NBL-79 series; this ore contains 0.035% uranium, a factor we have taken into account when calculating the thorium calibration values. A 50-g quantity of this ore was mixed with 850 g of serpentine fines and packed in a polyethylene container to constitute our thorium calibration standard.

Spectrometer-calibration runs were taken 8 days after packing these two mixtures, to ensure that any disturbance of equilibrium (loss of gaseous decay-series members) would be repaired, and could therefore not affect our results. We obtained the potassium standard spectrum from a homogeneous mixture by using the pure chemical compound, KCL. A 654-g quantity of this compound was packed in a polyethylene container to constitute our potassium calibration standard. The potassium calibration standard was also run at this time.

Each of the three calibration spectra is unique and shows characteristic peaks by which its identity can be verified in the mixtures encountered in sample analysis. Figures 4, 5, and 6 show calibration spectra from U, Th, and K, respectively. The uranium spectrum shows a relatively flat distribution up to channel 14, then a sharp drop followed by a prominent peak at channels 26 and 27, a broad peak in the low 50's, another broad peak in the 80's, and a sharp drop in the 90's. Thorium shows a sharp peak at channel 8 rising from a plateau that drops sharply beyond channel 14, a modest peak at channels 25 and 26, a broad peak in the low 40's followed by a dip in the 50's, and a relatively flat distribution in the 80's and 90's. Potassium shows a typical monoenergetic gamma-ray spectrum, with the single total absorption peak centered at channels 69 and 70, and with a nearly flat Compton distribution extending to about channel 60 but modified by a rise at the low-energy end by various scattering interactions. Figures 7, 8, and 9 are spectra from samples

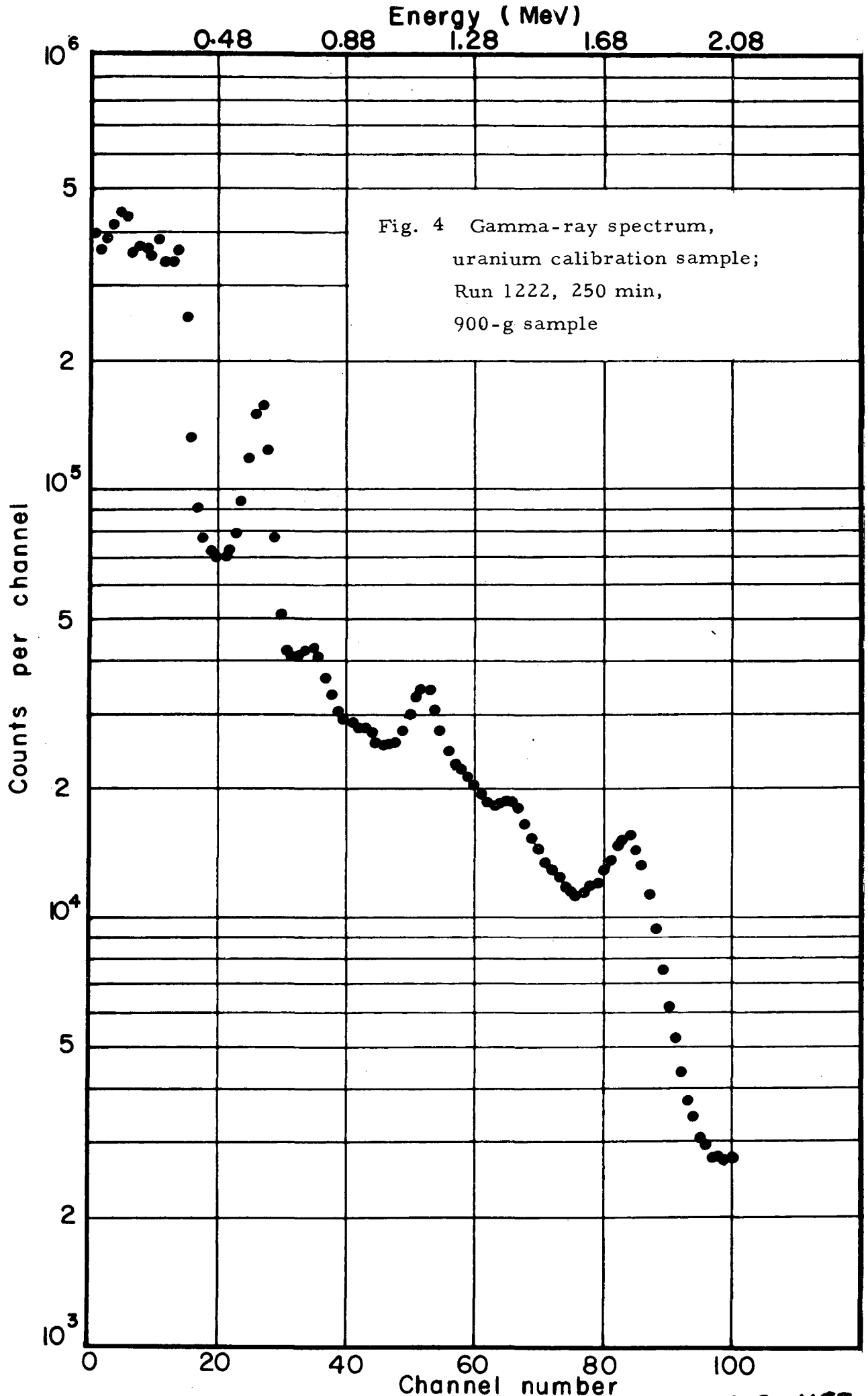

Fig. 4 Gamma-ray spectrum, uranium calibration sample; Run 1222, 250 min, 900-g sample

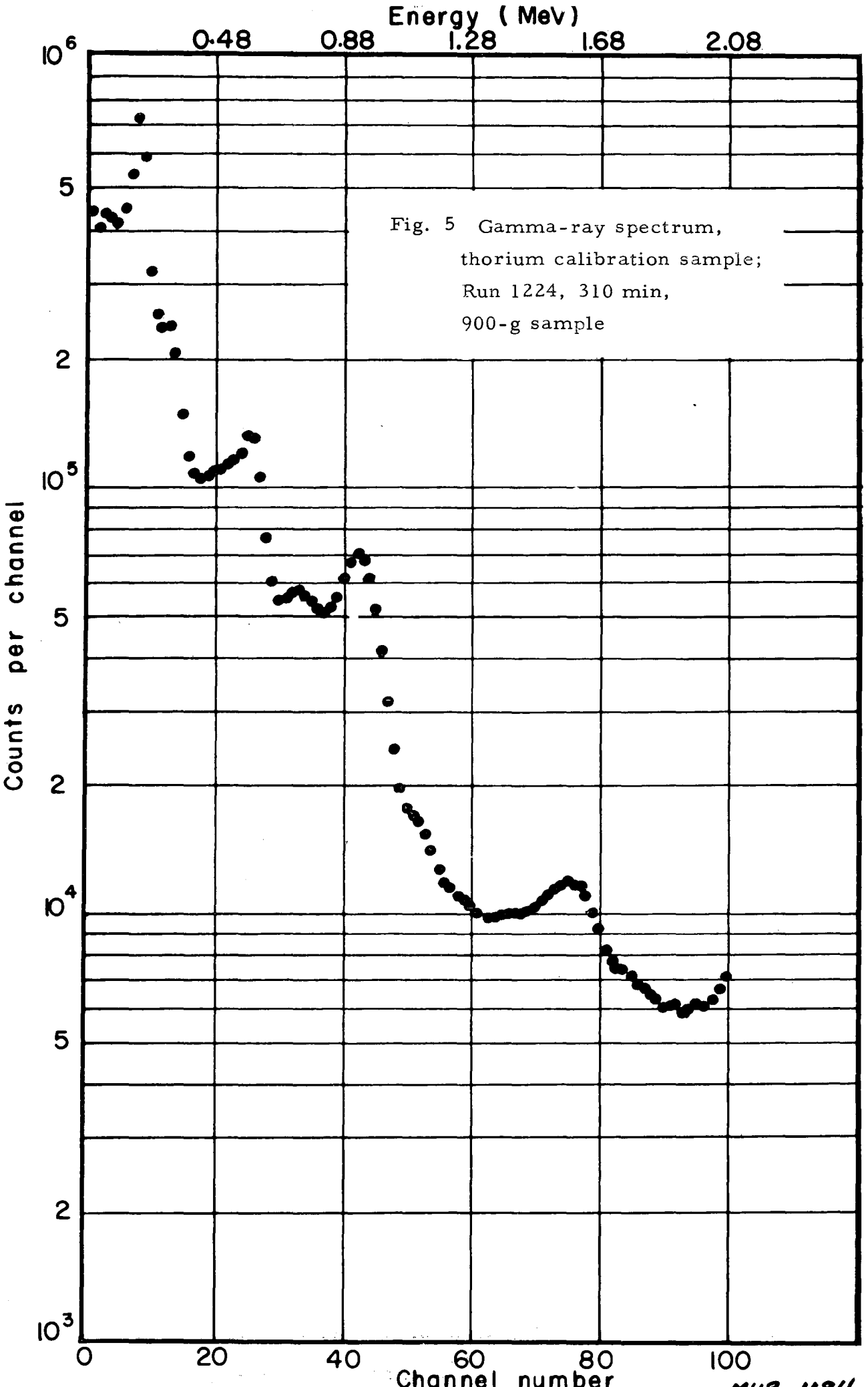

Fig. 5 Gamma-ray spectrum, thorium calibration sample; Run 1224, 310 min, 900-g sample

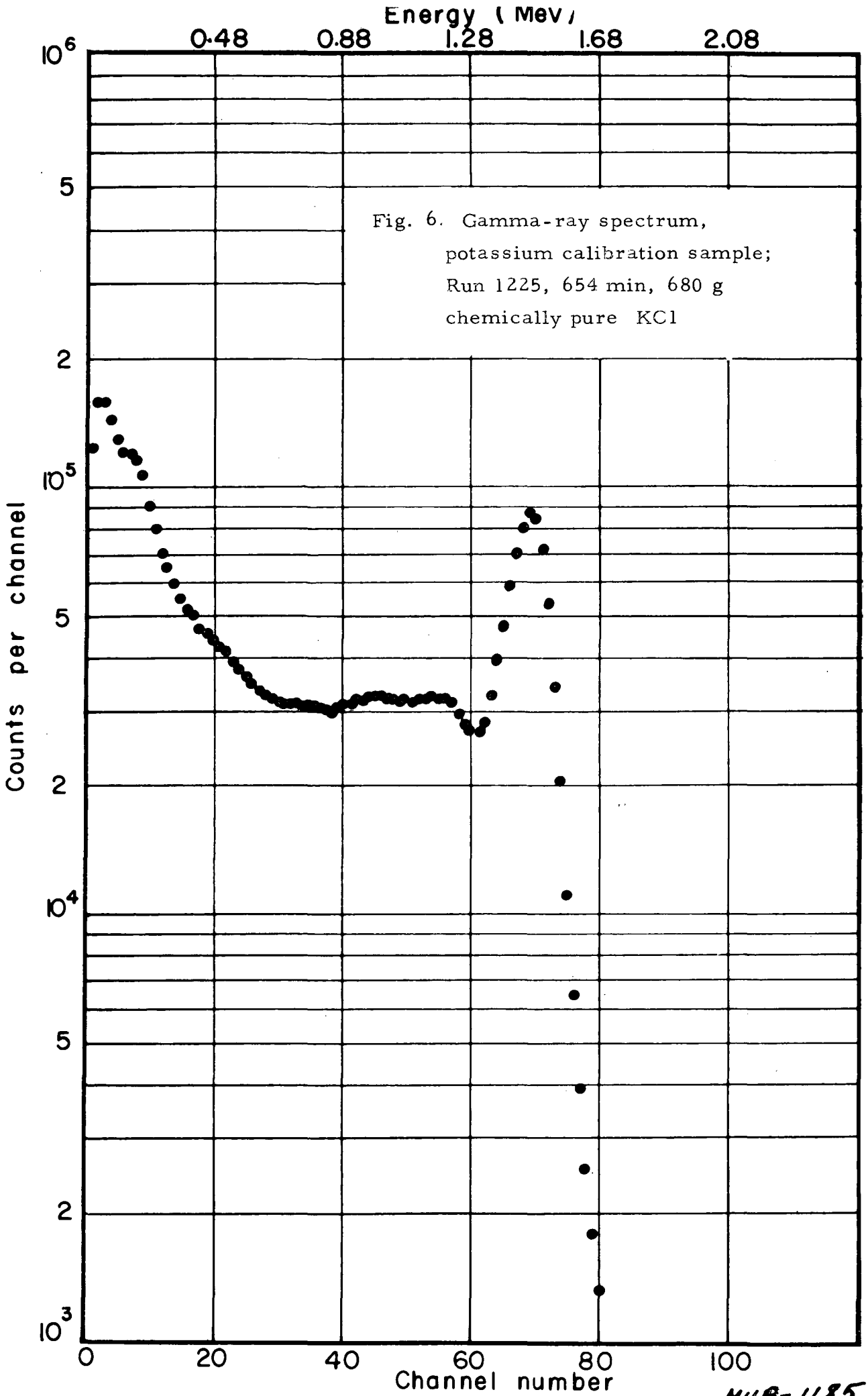

Fig. 6. Gamma-ray spectrum, potassium calibration sample; Run 1225, 654 min, 680 g chemically pure KCl

MUB-4185

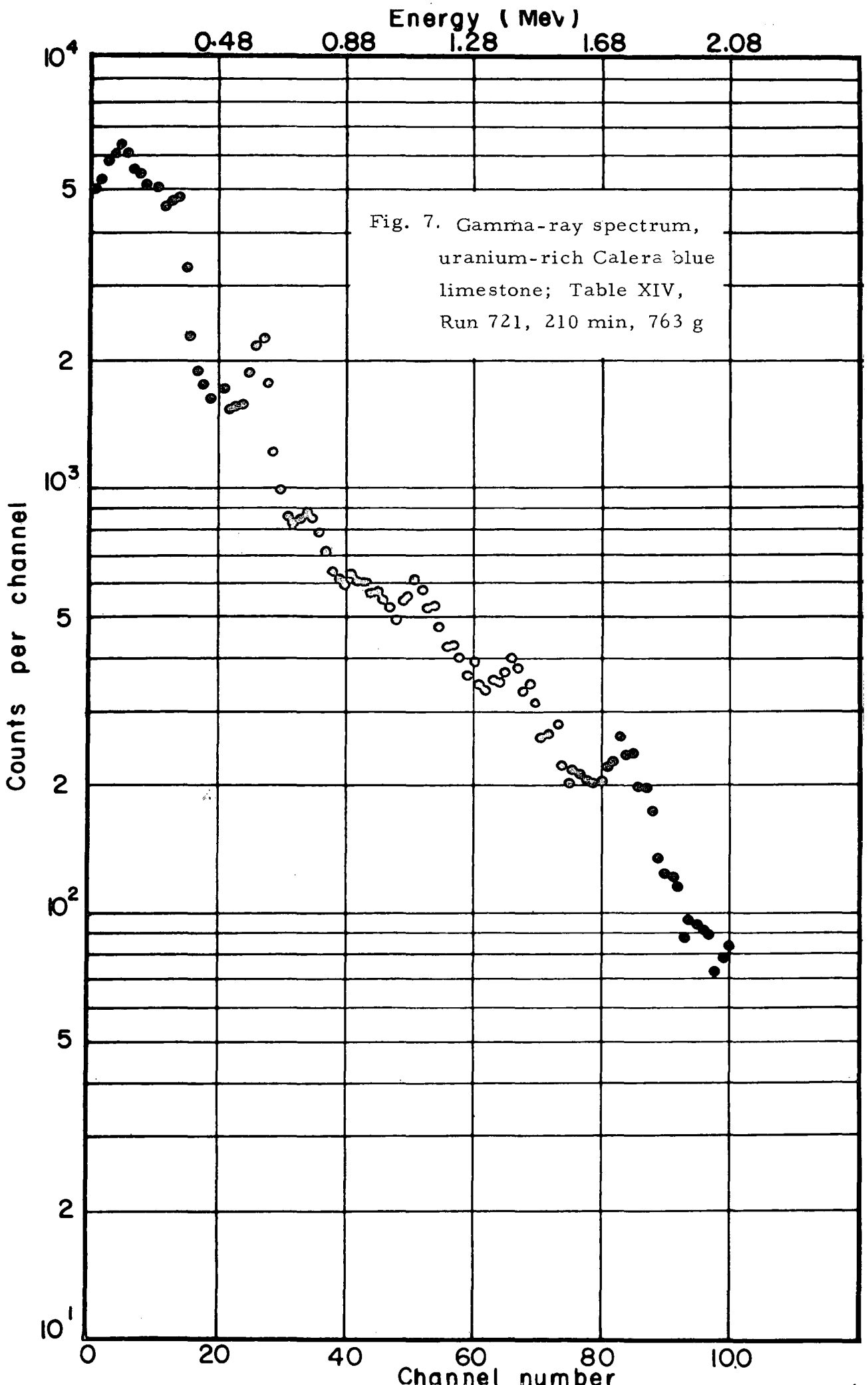

Fig. 7. Gamma-ray spectrum, uranium-rich Calera blue limestone; Table XIV, Run 721, 210 min, 763 g

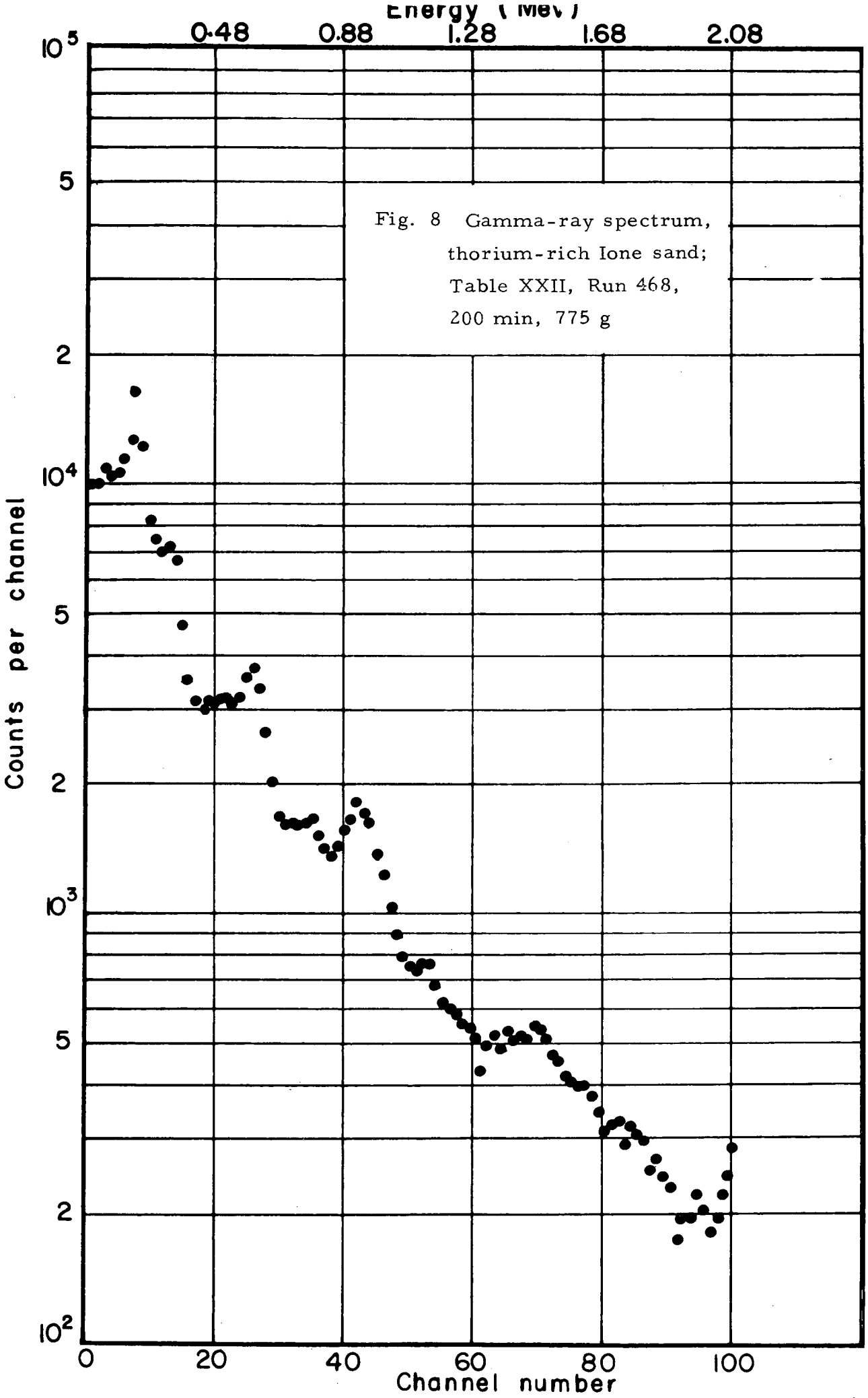

Fig. 8 Gamma-ray spectrum, thorium-rich Ione sand; Table XXII, Run 468, 200 min, 775 g

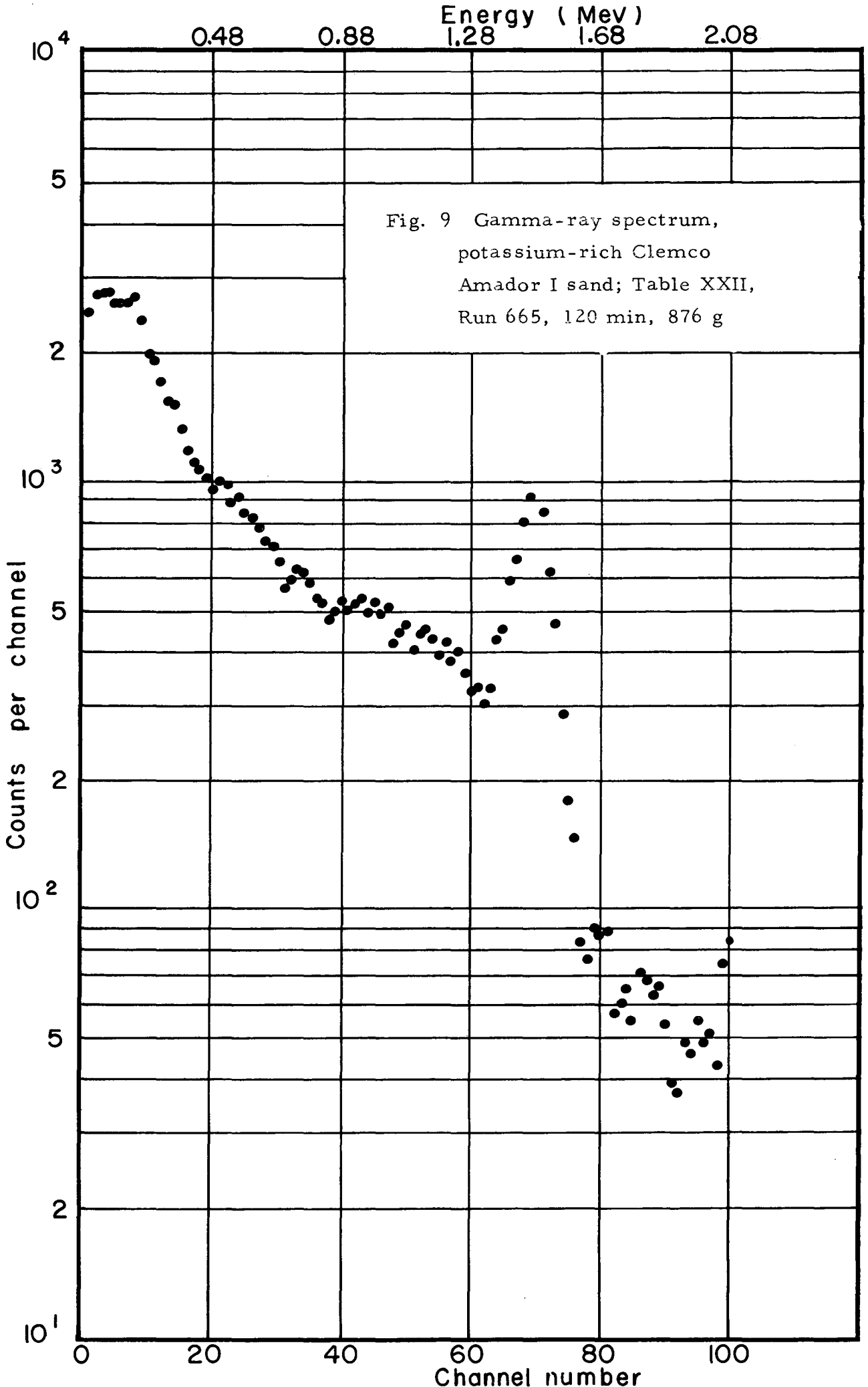

Fig. 9 Gamma-ray spectrum, potassium-rich Clemco Amador I sand; Table XXII, Run 665, 120 min, 876 g

of uranium-rich, thorium-rich, and potassium-rich rocks collected in the course of field examinations; BKG has not been subtracted from these three spectra. A comparison between these sample spectra and the calibration spectra is instructive.

Each of the three standards was counted until at least 200,000 counts were accumulated in each of the three intervals used for our calculations. We require such precision so that none of the parameters derived from these calibrations (subsequently used in solution of the equations) will contribute any appreciable error to the resultant analysis. In other words, only the statistical counting errors in the sample runs need to be taken into account when calculating precision of final results; such calculations are thereby simplified considerably. Table II lists the calibration parameters obtained from these runs. The last column at the right, Table II, lists spectrometer response in terms of counts per minute in the total observed spectrum from 1g of each of the three radioactive components.

No other naturally occurring gamma-ray emitters than U, Th, and K are likely to be encountered in sample analysis. However, we have detected fission-product activities (nuclear-weapon test debris) in some samples, particularly in ultramafic rocks. A few samples collected before September, 1961 showed two long-lived gamma-emitters from "old" fallout: Ce^{144} (a sharp peak in channels 3 and 4) and Cs^{137} (a sharp peak at channel 29). Samples collected since September 1961, particularly after the onset of winter rains, show several short-lived gamma-emitters from "fresh" fallout. Surface and near-surface materials are now contaminated to such an extent that we cannot always apply the methods described here without studying fission-product decay at the same time. (See Sec. VIII and Fig. 10 for a discussion of the recent fallout problem.)

H. Gamma-Ray Scattering Effects

Careful study of laboratory data taken on the lowest-activity materials, particularly the serpentines, points out one important problem associated with this sort of work: in general, the presence of any nonradioactive mass close to a detector will alter the count rate measured by the detector. When the detector is adequately shielded from external terrestrial radiation by a material that is not itself radioactive, as in our case, then the presence of the sample will invariably increase the observed count rate. The increase is expected to be small--only a few counts/min--and therefore can not be verified when high-activity samples are counted.

As the simplest description of the situation, we say that the sample acts as a scatterer of gamma rays, and that some of these scattered gamma rays are directed into and detected by our crystal. Most of these secondary gamma rays are produced from Compton interactions of primary gamma rays in the sample. The only concentrated source of radioactivity known to be inside the shield is the phototube glass envelope and the most important part of this envelope is the large flat photocathode end plate, which rests against the crystal window. Some of the gamma rays emerging from this glass pass through the crystal without interaction, and then interact in the sample to send Compton-scattered gamma-rays back into the crystal. Gamma rays scattered through such large angles by the Compton process are generally termed "backscatter" gamma rays, and produce a characteristic spectral shape that we would observe in the low-energy channels. All other

Table II. Calibration parameters for U, Th, and K.

	C_1 channel group 62 through 74	C_2 channel group 51 through 60	C_3 channel group 41 through 50	Total spectrum channels 1 through 100
U (250.0 min)				
Observed counts	207369	269163	270371	8334555
Normalized counts	1.0000	1.3016	1.3024	40.368
c/min-g of U	3170	4126	4128	127968
Th (490.0 min)				
Observed counts	214316	206147	713521	13912562
Normalized counts	1.0000	0.9107	3.6796	69.593
c/min-g of Th	740.4	674.3	2724	51526
K (654.0 min)				
Observed counts	704554	303684	315379	3844474
Normalized counts	1.0000	0.4261	0.4389	5.2858
c/min-g of K	2.9976	1.2774	1.3158	15.845

Compton scattered photons also have energy less than that carried by the primary photons. Thus, we expect the contribution from all Compton events to appear in the low-energy channels. We do not expect sharp structure in this spectrum, because Compton-scattered photons can have a wide distribution of energies when derived from a single primary-photon energy.

The serpentine spectra show no increase above background for the three energy groups used in the quantitative analysis. Yet, there is an increase noted above background when the entire 100-channel spectrum is used to assay sample activity. The excess counts are always at the low-energy end of the spectrum, in agreement with the proposed Compton-scattering effects.

We have attempted to determine the magnitude expected from such scattering interactions, by using a small uranium-ore source and a standard serpentine sample in normal counting position. When the uranium source is placed as close as possible to the phototube end plate, we note a count increase of about 2% when the sample is present, compared to the no-sample condition. If it is reasonable to treat the total background count rate in this fashion, then our serpentine activites are all 4 to 5 counts/min high; such a correction would reduce the detected activities of some serpentines below the point where they have any statistical significance.

I. Water Bearing Materials

Some of the lowest-activity materials we have attempted to assay, the serpentines, illustrate another aspect of neutron interference. The serpentines are hydrated ultramafic rocks, and contain about 10% water by weight; this quantity of water is effective as a moderator for fast neutrons. In the presence of a fast neutron flux, a serpentine sample then becomes a source of slow neutrons. It is important to point out that although our outer shield layer effectively absorbs the external fast neutron flux, the inner lead shield acts as a fast neutron flux generator via cosmic-ray interactions. The cosmic-ray produced fast neutron flux is small, to be sure, but it is not negligible in the present context.

Thermal-neutron capture cross sections for the major constituents of serpentine (Mg, Si, O, and H), and the NaI (Tl) crystal strongly favor capture in the crystal. Thus the crystal becomes slightly activated and reports information that appears to indicate radioactivity in the serpentine, while in reality these excess counts are due to the neutron-activation effects in the detector. Here again, the effect is measured in terms of a few counts per minute; however, the apparent sample activity is of comparable magnitude.

J. Lower Limit of Sensitivity

Our present lower limit for detection of radioisotopes is determined by several interrelated factors. We are, in a sense, limited by the length of count time, but a four-fold increase in count time is required to reduce the statistical standard deviation (error) by a factor of two. When count times of 2000 min are already employed, it is evident that simply increasing the count time may not be the most satisfactory way to increase detection sensitivity. It is also true that it requires a four-fold reduction in background to reduce the standard deviation by a factor of two, if count time remains fixed. No

such dramatic decrease in background can be expected beyond the point we have reached. We see that both count time and background magnitude are related to detection sensitivity in a "square-root" fashion; it requires large changes in either quantity to effect significant improvement in the desired direction.

However, the standard deviation decreases in direct proportion to the increase in sample count rate, other parameters remaining constant. Thus the most fruitful approach to improved detection sensitivity is to increase the sample count rate, either by presenting a larger sample mass to the detector, or by employing a more efficient (larger volume) detector. We cannot employ either of these alternatives while working in the confines of the small lead shield; however we will be able to take advantage of both soon when a large shield structure is completed.

Table III illustrates the performance of the present spectrometer-sample system in terms of the concentration of each component that produces 1 count/min in the total observed spectrum. We assume that a 1000-g sample is used, and that a count time of 1000 min is allotted so that the 1 count/min difference is statistically significant. It should be noted that we lose the ability to identify the radioactive components as this lower limit of detection is approached.

We are now able to assay potassium down to the range of 50 to 70 parts per million; in the large shield structure, and with a larger detector which views a greater sample mass, we should be able to reach the range of 1 to 2 parts per million potassium content. Improvement in detection sensitivity for uranium and thorium is expected to be of a magnitude similar to that quoted for potassium.

The problems discussed here are general for situations in which the sample count rate is but a small fraction of the background rate. We do not mean to imply that increasing count time and decreasing background rate are not worthwhile achievements; we want only to point out the relative magnitudes of the effect produced when these parameters are varied. Obviously, the background cannot be too low, nor can a longer count time fail to improve precision of results. However, these factors must be viewed in proper perspective, and in this context, sample count rate takes a pre-eminent position. Finally, so long as the background is high relative to the detected activity, this background must be known exactly if precise results are to be obtained. The background must remain extremely constant or, in our case, must be measured each time simultaneously when variations are encountered.

Table III. Least detectable quantities of U, Th, and K with present analysis system.

Radioisotope	Counts/min-g	Grams to produce 1 count/min	Concentration in 1000-g sample to produce 1 count/min
U in equilibrium	1.28×10^{5}	7.8×10^{-6}	7.8×10^{-9}
Ra in equilibrium	3.57×10^{11}	2.8×10^{-12}	2.8×10^{-15}
Th in equilibrium	5.15×10^{4}	1.9×10^{-5}	1.9×10^{-8}
K	1.58×10^{1}	6.3×10^{-2}	6.3×10^{-5}

IV. FALLOUT PROBLEMS

Our laboratory assay methods for U, Th, and K rest upon the assumption that no other gamma-ray emitters contribute counts to the three selected spectral intervals. These intervals have been selected to lie above the spectral region to which Ce^{144} and Cs^{137} ("old" fallout) contribute gamma-ray events. In fact, the computer analysis permits us to measure the amount of these fallout isotopes present in contaminated samples. We can take care of "old" fallout rather easily.

The fission products generated from nuclear weapons tests conducted since September, 1961, "fresh" fallout, are quite a different matter, however. This category of fallout can definitely interfere with the U, Th, and K laboratory analysis; it can interfere very seriously with field survey work, and so we feel the matter must be discussed here at considerable length.

At locations remote from the weapons test sites, fission products fall to earth mainly in the form of dust-sized particles. If rainfall is frequent, occurring several times per month, most fallout is brought down by this precipitation; conversely, if dry spells of several months duration occur, most fallout drifts slowly to the surface as dust, settling through the air. In most of California we have alternate periods for each mode of deposition every year: about 4-5 months of wet deposition and 7-8 months of dry deposition. Although the fallout particles are largely insoluble, their fate may depend strongly upon the mode of deposition. Dry deposition must be mainly and evenly on the surface, and can deliver a considerable burden to leaves of grasses, shrubs, and trees. Rainfall deposition, however, may purge activity from growing vegetation leaving it relatively clean, and may also scour fallout particles from other surface "dust-catching" facilities. Running water has great power to transport such small particles laterally; thus when rainfall is great enough to produce surface run-off, fallout particles are transported by this agent. For example, field work generally reveals higher activity in ditches and other low places where run-off has collected; laboratory analysis confirms that the excess activity is indeed fallout. Furthermore, fallout particles may be carried into cracks and crevices in weathered or broken rock formations. We have not usually found fallout in samples taken from greater than 2 feet below grade level in undistrubed material; however, it is not possible to generalize on the matter: each situation must be evaluated separately. In summation, the extent of fallout interference at a particular field site may depend on the length of time since the last rain, the intensity of the last rain, or perhaps whether trees and shrubs have leaves at the times in question.

These variables are of controlling importance for field work with an instrument of the type we use: a simple gross activity indicator. Lowder, et al. (1963) describe a technique to alleviate some of these difficulties. Our work with surface outcrops of ultramafic formations showed field count rates of 20-30 counts/sec before September, 1961. Since that time, count rates as high as 250 counts/sec have been observed at these same locations. Again, laboratory analysis shows the increase to be due to fallout. Field readings for higher activity formations have shown similar or even greater absolute count rate variations, although the relative differences here are less. Figure 10 shows computer-derived spectra for a surface soil sample collected at El Cerrito, California in late October 1962. The background-corrected observed

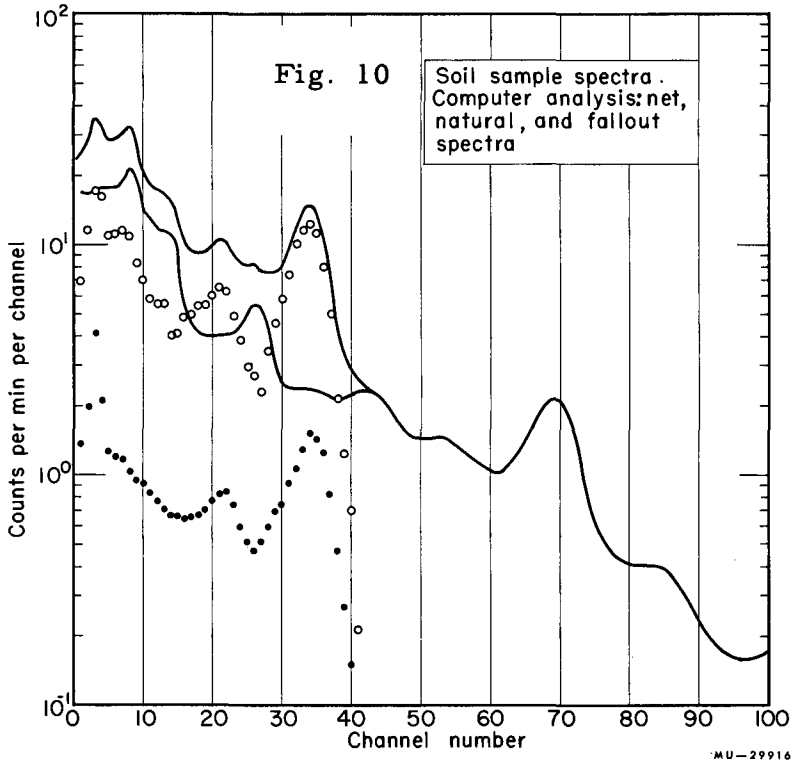
Fig. 10
Soil sample spectra. Computer analysis: net, natural, and fallout spectra
Counts per min per channel
Channel number
MU-29916

spectrum appears as the top solid curve on this figure. The 100-channel synthesized natural activity spectrum is the next lower curve, and is seen to merge with the observed spectrum beyond about channel 40. The "fallout" spectrum appears next as a set of points; it is a true fallout spectrum and extends only to channel 40. The computer shows 383 counts/min natural activity and 276 counts/min fallout for this sample. For comparison purposes we show a fourth spectrum, appearing at the bottom of Fig. 10; it is the spectrum from dried weeds in a ditch, collected at Felton, California in April 1962. The only detectable activities in the weed sample are fission products; the soil "fallout" spectrum is seen to be very similar. This figure also illustrates the sort of information we derive from the computer analysis.

For field measurements over unfamiliar formations, we cannot now assign a natural activity count rate; we might easily be in error by a factor of 2, or by nearly a factor of 10 if ultramafics are at hand. A qualitative test for the seriousness of the fallout problem can be performed by digging a pit for the detector to get it below grade level. When fallout is a problem, the pit position will show a lower count rate than the normal surface position. We have not yet tried to make this test quantitative, but have firmly established its qualitative validity.

At the present time we are forced to rely upon laboratory analysis, even to interpret the simple data collected in the field; but the laboratory job is by no means clearly resolved for all samples. We now recognize two kinds of "fresh" fallout situations. The first case includes all samples that show La^{140}, a 1.60 MeV gamma-ray emitter with an effective half-life of about 2 weeks; samples are likely to be in this class if they have been collected from the surface shortly after a rain and within a few weeks after large-scale atmospheric testing. The U, Th, and K assays are not valid for these samples.

The second class includes the first-class samples after about a month decay time, and all other samples except those taken from deep underground or from other sufficiently protected sites. These samples may contain the medium-lived fission products Ce^{144}, Rh^{102}, Ru^{103}, Ru^{105}, Rh^{105}, Zr^{95} - Nb^{95}. Several of these isotopes have complex spectra, but they combine to show three prominent peaks: Ch 3 to 4, Ch 18 to 20, and Ch 33 to 35 (Zr^{95} - Nb^{95}). Such samples may also contain Cs^{137}, but its peak at Ch 29 is usually masked by the Zr - Nb peak in the low 30's at this early age of fission products.

We can perform the U, Th, and K assay for these samples. If the Zr-Nb peak is very intense, its upper edge may contribute slightly to the Ch 41 to 50 interval, and thereby produce an artificially high Th assay. However, this difficulty seems not to be serious in most cases, and is mainly a problem for those surface samples we collect explicitly for fallout measurement. It must be noted that "very intense" is a relative term as applied to the Zr - Nb peak, and ultramafic materials may all show trouble here because their natural activity is so low.

Results from our computer problem have begun to show a consistent over-estimate of uranium assay in some of our surface soil samples. These samples contain a significant fallout component. It is possible that some of the relatively low-abundance high-energy gamma rays from Rh^{102} cause this

error. Additional computer analysis of such spectra must be accomplished before we can learn the truth of this matter.

The items discussed here may be only of short-term value; cessation of atmospheric nuclear weapons testing would ensure that these problems virtually disappear after a year or so. However, we can only speculate on the testing schedule, and these problems are certainly with us right now. It is generally true that most of the fallout does stay at or near the surface, but one cannot be certain about this matter. If most fallout at a site does lodge near the surface, then field scanning is subject to potentially great error, while sub-surface collection for laboratory analysis is in a more favorable circumstance. Finally, anyone who has worked in the field will appreciate the difficulty of "mining" deep enough into a weathered surface outcrop to obtain a sample that is almost certainly free of fallout.

V. COMPARISON OF FIELD AND LABORATORY ANALYSES

A comparison of field-survey measurements with laboratory spectrometer analyses shows that the two kinds of data agree generally. There are some exceptions. Among the medium- to high-activity sample materials, these disagreements can usually be attributed to some constraint in the sampling environment: lack of uniformity of sample area, smallness of sample volume, or recently, the presence of fresh fallout.

There is often very poor agreement between the two kinds of data for analyses of the materials with lowest-activity--the ultramafic formations. There is good reason for this lack of agreement. For example, when we examine a surface deposit of serpentine, the portable instrument readings represent a relatively large amount of material, some of which may be foreign to the serpentine itself. However, a sample collected for laboratory study will contain only serpentine and no foreign materials, when we wish to assay serpentine activity. Therefore, field and laboratory results might disagree. Nearby outcrops of high-activity rocks can influence field measurements, but would not affect laboratory data. Furthermore, in many cases the field instrument detects almost no radiation from the serpentine, but records mainly airborne activity and internal contamination. We cannot expect to distinguish a small increment to this base count rate with much precision, especially when the base count rate may vary with time or location. Laboratory conditions are much more favorable for determining these small increments accurately. With the field instrument we can always identify the ultramafic formations by their very low activity (except where there is appreciable "fresh" fallout); it is just that we cannot distinguish the lowest from the low in the field.

Higher activity rock types tend to show better field vs laboratory activity correlations. (This is illustrated in Fig. 15 where a fair correlation exists with cement-plant limestones, and a good correlation exists with cement-plant "shales.")

VI. SOME RESULTS OF OUR STUDIES

During the past two years we have accumulated gamma-ray spectrographic data from over 1500 soil and rock samples. The impetus for the rock-sample study was furnished by the quest for low-radioactivity aggregate materials for our low-background counting room; the soil samples were collected during periodic fallout surveys in the San Francisco area. Soil samples were subsequently analyzed for the natural component of gamma radioactivity. Rock sample data are extensive enough so that gamma-radioactivity characteristics of several widely varying rock types can be compared; these include Oregon basaltic flows, central California ultramafics, California carbonate rocks, siliceous sands, and vein quartz.

An example of the practical application of our techniques is that of the analysis of portland cement raw materials and finished products. Our cement data is clearly of value to persons interested in low-background concrete ingredients; it should also be useful to persons in the cement industry concerned with raw-material ingredient concentrations in mill feed, and with the ultimate distribution of raw-material chemical components in produced cements.

A. Volcanic Rock

Fifteen samples were collected from the sequence of Tertiary and Recent volcanic flows, tuffs, and gravels, cropping out along State Highway 20 which traverses the Cascade Mountains west of Bend, Oregon. The sample with the lowest natural activity, 0.180 counts/min-g consists of olivine basalt collected from the vicinity of Santiam Summit. The highest activity, 0.815 counts/min-g, occurs in a sample of feldspathic tuff collected on the western slope of the Cascades. Field counting rates average 234 counts/sec with the extremes of 500 counts/sec over the feldspathic tuff and 150 counts/sec over stockpiled basalt cinders.

Ten samples (1 through 10 on Table IV) were taken from olivine basalt and andesite which form the summit and east slope of the Cascades, an area described by Williams (1957). These lavas range in age from Pliocene to Recent with the oldest, corresponding to samples 7 through 10, having undergone glaciation. Average isotope concentrations for the ten samples follow: uranium, 0.90 ppm; thorium, 1.61 ppm; potassium, 0.56%.

The remaining five samples listed on Table IV were collected in older (Oligocene to Pliocene) volcanic rocks which crop out on the west slope of the mountains. Among these formations the Miocene Stayton lavas, corresponding to sample 13, are considered to correlate stratigraphically and lithologically with the Miocene Columbia River Basalt; both are low in olivine. The five samples from the western Cascades average 1.17 ppm uranium, 3.18 ppm thorium, and 0.74% potassium.

When the plots of K, U, and Th concentration vs overall counting rate are compared (Fig. 11), it is apparent that thorium is the principal determinant in the radioactivity of the volcanic-rock samples. Uranium and potassium concentrations also follow count rate variation, but to a lesser extent than for thorium.

Table IV. Gamma-ray spectrographic evaluation of Oregon Volcanic Rock

Description	Concentration U (ppm)	Concentration Th (ppm)	Concentration K(%)	Field counting rate[a] (counts/sec)	Ratio Th/U	Natural activity counting rate (counts/min-gm)
1. Andesite pebbles, Metolius Junction	1.16	1.43	0.56	195 avg. over surf. 160 surrounded	1.23	0.309
2. Lava Butte cinders	1.39	3.58	1.08	250	2.58	0.531
3. Pilot Butte cinders and soil	0.625	2.25	0.66	175	3.60	0.300
4. Basalt, Santiam Junction	0.85	2.00	0.59	175	2.36	0.304
5. Cinders, Santiam Junction Stockpile	0.62	0.78	0.65	150	1.26	0.223
6. Basalt, vicinity, Laidlaw Butte	1.87	2.37	0.28	190	1.27	0.406
7. Cinders, Suttle Lake	0.85	1.23	0.55	225	1.44	0.258
8. Solid basalt, Suttle Lake	0.70	0.70	0.41	185	1.00	0.190
9. Vesicular basalt, Santiam Summit	0.32	0.96	0.38	230	2.99	0.218
10. Solid basalt, Santiam Summit	0.57	0.79	0.42	230	1.39	0.180
11. Feldspathic basalt, Tombstone Pass	0.41	0.96	0.45	215	2.36	0.173
12. Feldspathic tuff, Rooster Rock	2.04	5.96	1.56	500	2.92	0.815
13. Fine-grained basalt, ≈1 mile east of confluence of Middle and South Santiam Rivers	0.56	2.28	0.34	240	4.12	0.242
14. Columnar basalt, ≈2 miles west of Cascadia	0.98	3.63	0.68	250	3.72	0.419
15. Volcanic pebbles	1.84	3.07	0.68	300	1.67	0.498
Average values	0.99	2.13	0.62		2.26	0.338

[a] includes fallout component

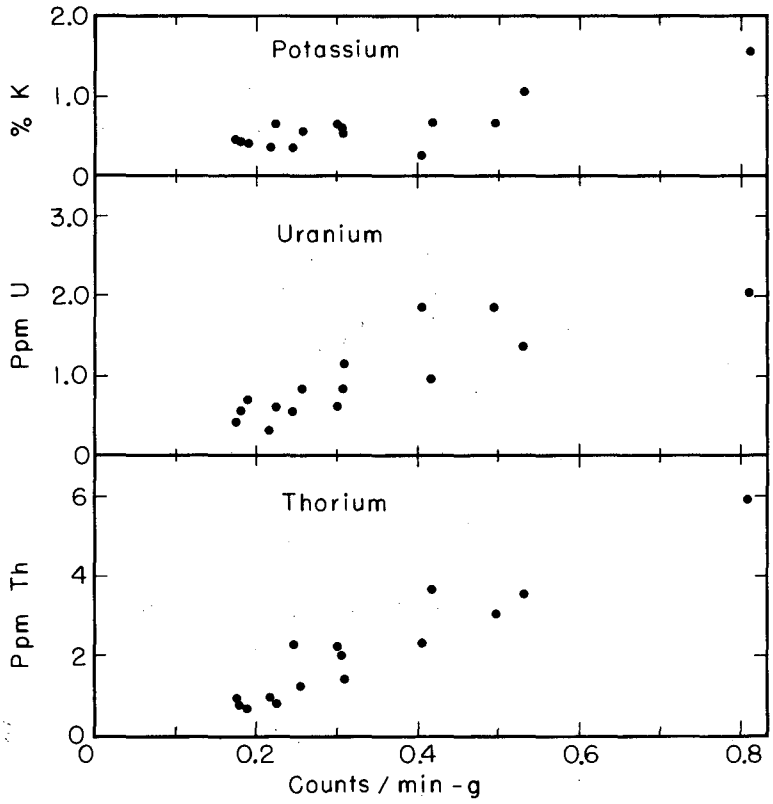

Fifteen Oregon basalt samples

MU-29925

Fig. 11

It is interesting to note that the feldspathic tuff, considered to be the most acidic member of this volcanic sequence, is highest in U, Th, and K concentrations and is also highest in overall count rate, while the basic basalts of Santiam Summit have the lowest radioisotope concentrations and the lowest overall count rates.

Of further interest would be the possibility of a correlation between the alkalinity of the plagioclase feldspar and the radioactivities of these and other basalts.

B. Ultramafic Rocks

Serpentinized ultramafic rocks were considered those most likely to fulfill the low background requirements of aggregate for our counting facility. Possible sources of serpentine and magnesite in Central and Northern California were examined and sampled, with samples being subjected to gamma-ray spectrographic analysis. Average values for 26 selected "uncontaminated" samples follow: overall counting rate, 0.0197 counts/min-g, concentrations: K-0.001%, U-0.11 ppm, Th-0.07 ppm. Field portable scintillation counter readings corresponding to 22 of the above samples averaged 37 counts/sec. All readings were made prior to fallout in the autumn of 1961, so that Cs^{137} was the predominant fission product present.

Serpentine may contain higher uranium concentrations than unaltered ultramafic rocks (Davis and Hess, 1949), and it is therefore possible that pure periodotite or dunite may contain less radioactivity than we have measured in our serpentines. Economics dictated that we locate a source of aggregate fairly close to Berkeley; sources of pure periodotite or dunite were out of range on this basis. We have not yet obtained good data from such unaltered formations, but plan to do so in the near future. Samples of Forsterite brick, both in the form of raw material and finished product, have been assayed; results show these samples to contain considerably more radioactivity than our serpentines. The source for this product is in an unaltered dunite from North Carolina; however, no special effort was made to keep radioactive contamination from the samples we received prior to receipt. The high radioisotope content may be due to this factor. It is also possible that ultramafic rocks in other parts of the U. S. may not have the low radioactivity of those on the West Coast.

The marked contrast between the low activity of ultramafic rocks and the higher activity of adjacent rock types was evident wherever field readings were made. A good example is the contrast at the Phoenix Asbestos Mine near Napa, California: a reading of 300 counts/sec was observed over sandstone, while 10 feet away, down a steep incline across the sandstone-serpentine contact, the reading over serpentine was 30 counts/sec.

The effect of an adjacent high-activity rock type on serpentine field count rates is illustrated in the Sierran foothills, where Tertiary latite lava flows overcap Mesozoic serpentine. At one location field readings were 1400 counts/sec over the latite, and 160 counts/sec over a nearby serpentine outcrop. Laboratory analysis indicates that the serpentine is virtually free of radioactivity, showing that the nearby latite produced the abnormally high reading over the serpentine.

There are areas near the coasts of California, Oregon, and Washington where similar low-activity ultramafic rocks constitute the bulk of surface outcrops. These areas should show an unusually low terrestrial component of natural radiation; in our experience this is always the case, wherever readings have been taken. The extremely low radioactive content of these formations, and the close proximity of some of them to quite high-activity formations provides a fascinating opportunity for study. In the absence of fallout, only cosmic rays and airborne activity contribute to the radiation field, save for contamination within a detector and people in the vicinity. Such locales should provide very favorable circumstances for the study of airborne radioactivity and low-energy cosmic ray phenomena. It is an interesting speculation that the lowest-intensity natural background outside the ice-covered polar regions might be found over an extensive outcrop of ultramafic rocks along the Pacific Coast, where the prevailing westerlies, having traversed thousands of miles of open ocean, should be devoid of radon. The radiation intensity at such a place should be lower even than that observed over the ocean.

C. Limestone and Dolomite Samples

In the course of an investigation of cement-plant raw materials and possible low-background aggregates we have subjected samples of California carbonate rocks to gamma-ray spectrographic analysis. In these samples (28 of which are considered fairly "pure" carbonate rocks, i.e., with little or no interbedded shale material) uranium predominates over thorium and potassium as the principal contributor of radioactivity. This is illustrated by the frequency-distribution histograms in Fig. 12, which show that in over 40% of the samples uranium is responsible for 90 to 100% of the total counting rate. This predominance of uranium can be explained in part by the fact that the activities ratio of U: Th: K in counts/min-g of element is 128,000: 51,500:16. However, the absolute abundance of uranium over thorium, and the scarcity of potassium in the carbonate rock samples is illustrated by the maximum, minimum, and average values tabulated below, and the plots of U and Th concentrations versus overall counting rate in Fig. 13.

	Concentration			Ratio	Overall counting rate due to natural radioactivity, (counts/min-g)
	U (ppm)	Th (ppm)	K (%)	Th/U	
Maximum	4.87	1.80	0.28		0.601
Minimum	0.03	——	——		0.023
Average	1.25	0.35	0.05	0.28	0.186

Gamma-ray spectrographic evaluations of carbonate rocks are listed on Table V.

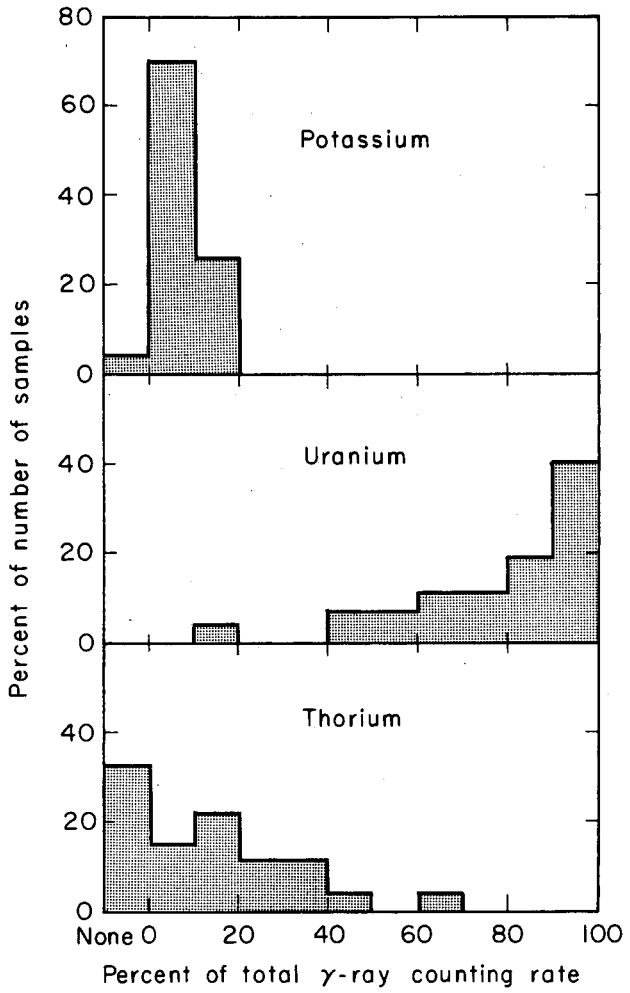

Frequency distribution of contributions of K, U and Th to the gamma-ray counting rate in 28 carbonate-rock samples

MU-29924

Fig. 12

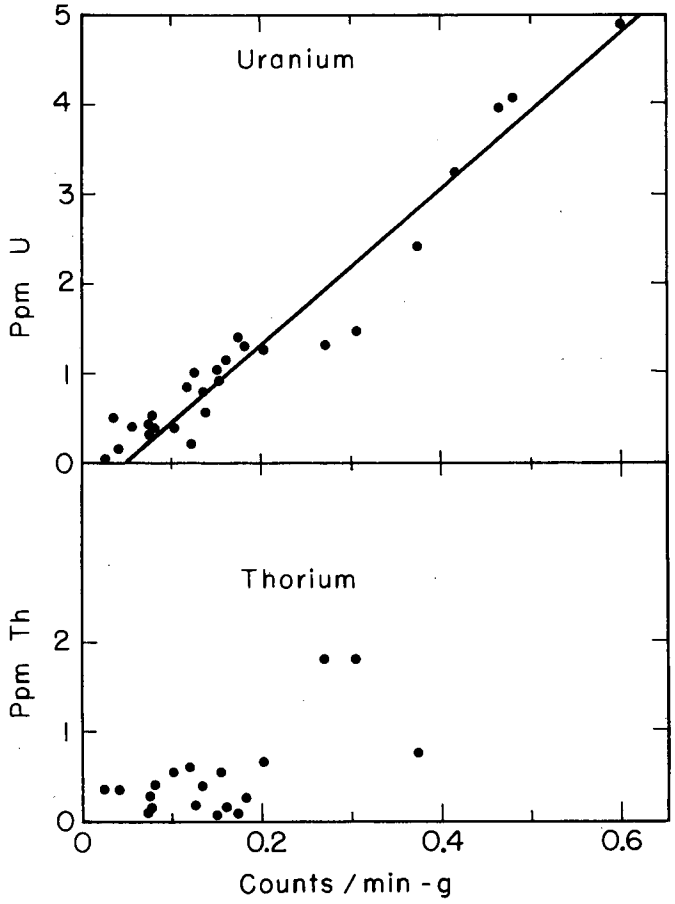

Limestone and dolomite samples

MU—29926

Fig. 13

Table V. Gamma-ray spectrographic evaluation of carbonate-rock samples.

Run No.	Limestone formation	Contribution to total γ-ray spectrum (counts/min)			Concentration			Overall counting rate (counts/min-g)	Field counting rate (counts/sec)
		K	U	Th	K (%)	U (ppm)	Th (ppm)		
478	Calera, white	4	3	14	0.03	0.03	0.36	0.023	50
721	Calera, blue	2	387	-	0.02	3.96	-	0.465	250
588	Gabilan	10	41	23	0.08	0.39	0.55	0.101	-
590	Sur series	4	122	3	0.03	1.03	0.07	0.149	-
609	Kernville (some biotite)	11	131	26	0.09	1.27	0.65	0.201	120
611	Kernville (biotite-free)	3	45	4	0.03	0.44	0.10	0.076	80
604	Bean Canyon high grade	12	145	-	0.09	1.30	1.80	0.268	-
634	Sparkuhle contact	21	159	3	0.15	1.38	0.07	0.175	140
618	Sparkuhle	4	120	23	0.02	0.80	0.39	0.135	70
619	Sparkuhle, dolomitic	1	33	-	trace	0.26	-	0.034	70
620	Shay-Klondike	6	42	16	0.04	0.40	0.39	0.080	70
659	Black Mt. conglomerate	32	270	33	0.23	2.40	0.76	0.376	120
642	Black Mt., low MgO	41	175	84	0.28	1.46	1.78	0.304	140
666	Furnace white	9	25	28	0.07	0.22	0.62	0.121	40
677	Furnace blue	1	50	12	trace	0.45	0.28	0.074	70
617	Jurupa, low MgO	1	90	-	trace	0.83	-	0.117	50
676	Chino, footwall	-	541	-	-	4.87	-	0.601	220
684	Chino, high lime	7	377	-	0.04	3.23	-	0.416	190
678	Calaveras, high grade	2	55	-	0.02	0.39	-	0.054	60
687	Calaveras, dolomitic	5	37	13	0.03	0.31	0.28	0.074	30
732	Calaveras, dark	3	94	7	0.03	1.00	0.19	0.127	-
818	McCloud	-	126	6	-	1.14	0.14	0.161	-
808	Calera, Rockaway Beach	3	150	11	0.02	1.30	0.24	0.182	-
508	Gabilan dolomite, Natividad	9	25	21	0.05	0.16	0.33	0.041	80
800	Calaveras, dolomitic, Sonora	1	62	7	trace	0.51	0.14	0.077	-
864	Calaveras white dolomite	10	108	27	0.07	0.91	0.56	0.151	-
827	Calaveras gray dolomite	7	113	-	0.05	0.57	-	0.137	-
826	Calaveras white limestone	1	376	-	trace	4.05	-	0.479	110
	Average values				0.05	1.25	0.35	0.186	103 (for 19 samples)

In their discussion of thorium and uranium in carbonate rocks Adams and Weaver (1958) state that about 80% of the uranium in limestone is bound up in the calcite crystal lattice, while thorium and about 20% of the uranium occur in the acid-insoluble detrital fraction. Therefore, the purity (Mg- or Ca-carbonate content) of a limestone or dolomite should vary inversely with its thorium content as well as with the concentration of potassium, whose presence is due primarily to small amounts of clay and authigenic feldspars. A carbonate rock with a predominance of uranium over little or no thorium or potassium could be considered high purity as opposed to one with appreciable Th and K, indicating the presence of clay and detrital minerals.

D. High-Silica Material

In our investigation of possible sources of low-background aggregates, several commercial sources of quartzose, high-silica sand were investigated in Central California in hope that suitable material for the minus 3/16 in. fraction could be obtained. We also investigated sources of quartz for possible use in the coarser aggregate sizes. The results of the radiometric examinations of these materials are listed on Tables VI and VII.

With the exception of the Blackhawk silica sand (considered "Ottawa Standard Sand" by laboratories in the Bay Area) the sand samples show generally high radioactivities when compared with the quartz samples. This can be attributed to the varying concentrations of grains of K-feldspar and resistate minerals in the commercial sands, while vein quartz in its pure form has little or no radioactive contaminants.

An interesting comparison is that between quartz and quartzite cobbles found in old placer tailings at Michigan Bluff, California. The quartzite is the product of the metamorphism of quartzose sandstone. Radiometric evaluation of the quartzite (Table VII) indicates the presence of K, U, and Th in amounts similar to those in a high-grade silica sand, while the quartz cobbles derived from stream-transported vein material are essentially free of radioactivity.

E. Portland Cement Study

The usefulness of gamma-ray spectroscopy is demonstrated in a search we conducted for a portland cement adequately low in radioactivity for use in the concrete of our low-background counting facility. The results of this study are fully reported by the authors in UCRL-10475. To determine the sources of radioactive contamination of cement we visited all operating California plants and their adjacent quarries, sampled all raw materials and subjected them to gamma-ray spectrographic analysis. As a result we determined that uranium, the principal contributor of radioactivity to the limestone, is also the principal contributor to cement's activity, while thorium, the principal contributor in the siliceous - "shale" and aluminous-clay raw materials, is the secondary contributor in California cements.

With one exception "shale" material at California plants has a higher radioactivity than the corresponding limestone. The histogram in Fig. 14 illustrates the higher activity of "shale" when compared to limestone. Laboratory counting rates for "shale" average 0.900 counts/min-g, while limestone

Table VI. Gamma-ray spectrographic evaluation of sand samples.

Run No.	Description	Counting rate (counts/min-g)	Concentrations			Contributions to total gamma-ray spectrum (counts/min)		
			U (ppm)	Th (ppm)	K (%)	K	U	Th
899	Nortonville sand	0.610	0.98	3.82	1.89	233	98	154
645	Corral Hollow sand, in old coal adit	0.694	1.39	7.12	1.03	164	180	370
646	Corral Hollow sand, tailings dump	0.823	2.36	9.66	0.22	29	251	414
648	Corral Hollow sand, pile alongside hopper	0.548	1.07	5.24	1.32	184	120	237
649	Corral Hollow sand, hopper near adit portal	0.655	1.39	5.04	1.53	235	174	253
468	Ione sand, Buena Vista pit	1.219	2.96	17.28	0.15	19	294	690
665	Clemco Amador I sand	0.415	0.21	1.35	2.01	275	24	61
673	Clemco II silica sand	0.123	0.62	0.74	0.06	10	82	40
685	Monterey sand	0.785	0.03	3.96	3.21	520	4	209
672	Sierra Gem No. 12 sand	0.097	0.31	0.56	0.15	23	39	28
580	Blackhawk (Ottawa, Ill.) silica sand	0.047	0.19	0.37	-	-	26	20
664	Felton-Santa Cruz sand	0.621	0.74	1.40	2.82	406	87	66
806	Contra Costa Ready-Mix Co. "Top Sand"	0.306	0.91	2.06	0.58	92	117	107
532	Clemco No. 24 Silica Sand	0.088	0.19	0.96	0.06	10	27	55

Table VII. Gamma-ray spectrographic evaluation of quartz samples.

Run No.	Description	Counting rate (counts/min-g)	Concentrations			Contributions to total gamma-ray spectrum (counts/min)		
			U (ppm)	Th (ppm)	K (%)	K	U	Th
874	Michigan Bluff, Calif. placer quartz cobbles	0.011	-	-	0.02	3	-	-
797	Michigan Bluff, Calif. quartzite cobbles	0.151	0.47	1.46	0.14	17	46	57
875	Crushed "Clear Cat" vein quartz	0.020	0.11	-	-	-	11	-
885	Hornitos, Calif. vein quartz, with pyrite, and some mariposite	0.012	-	-	0.05	6	-	-
815	Hornitos vein quartz	0.0045	-	-	-	-	-	-
907	Rogue River, Oregon quartz, (crushed by Industrial Minerals and Chemical Co., Berkeley)	0.018	0.08	0.12	-	-	9	5
873	Vein quartz, Coulterville, Calif.	0.001	-	-	-	-	-	-
872	Iron stained, weathered, vein quartz, Coulterville, Calif.	0.006	-	0.05	trace	1	-	2

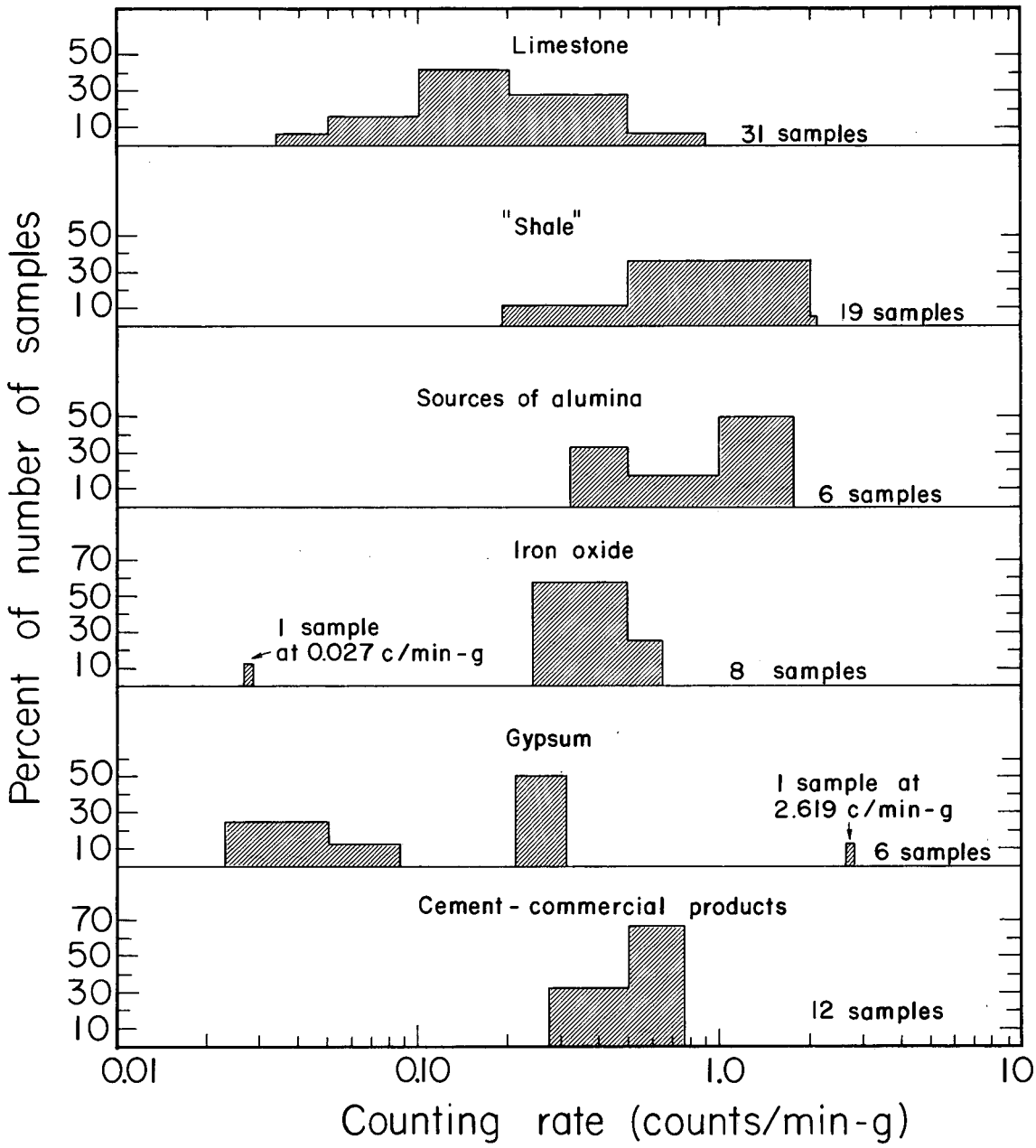

Fig. 14 Frequency distribution of overall gamma-ray counting rates of cement raw-material ingredients.

MUB-1405

averages 0.231. Field scintillation-counter readings average 314 counts/sec in "shale" deposits, 103 counts/sec in limestone. Plots of field vs laboratory counting rates for limestone and "shale" (Fig. 15) indicate good correlations where field count rates are representative of the material scanned.

On the basis of our California cement raw-materials study we can state that, with some exceptions, limestone is the ingredient primarily responsible for determining the radioactivity of the finished product. Limestone usually makes up about 80% of the kiln feed at cement plants, while "shale" material comprises only 10 to 15%. However, at plants where "shale" has an activity 3 to 4 times that of the limestone, "shale" achieves parity, or predominates in contributing to the cement's radioactivity. This is the case at some plants in Southern California where micaceous schists and metasediments are the sources of "shale." We emphasize, though, that low-activity cement can never be made from high-activity limestone. We expect that most workers who care about cement activity are attempting to obtain a low-activity product; thus the importance of limestone is evident.

California cement plant "shale" materials are derived from widely differing rock types, depending upon plant location. Besides the micaceous schists and metasediments mentioned above, Southern California plants also draw on quartzites, lateritic clay, and interbedded shales, while plants in the northern part of the state utilize andesite, diatomaceous shale, phyllite, altered volcanics, and lateritic clay.

In other sections of the United States, it appears that limestones play a more dominant role in determining the radioactivities of their respective cements. Though we have not counted the raw materials from these plants we suspect that a correlation exists between the counting rates of cements and the most utilized limestones. This is illustrated in Table VIII.

An example of the usefulness of gamma spectroscopy in determining the distribution of radioactivity in a cement plant's raw materials and finished product is illustrated by the study we conducted on samples furnished by the Lafarge Cement Company of Vancouver, British Columbia. Along with the samples, the company sent us data indicating that there is an overall weight loss (or ignition loss) of 36.4% between kiln-feed slurry and clinker, due to volatilization during calcining. Our spectrographic evaluation of calculated kiln feed and cement product indicated that during clinkerization, the K content is little changed; U, Th, and overall counting rate are increased by 38, 39, and 36% respectively. These increases are quite close to the overall ignition loss of 36.4%. This suggests that at Lafarge, U and Th are concentrated during calcining, and are not among the volatile constituents of clinkerization. The K content remains unchanged during calcining, indicating that K is volatilized in an amount equal to the overall ignition loss.

The following steps, illustrated in Table IX, were performed to achieve the above results:

(a) calculate the percentages of raw materials in the finished product (clinker plus gypsum) by applying ignition-loss percentages to the amounts of raw materials in the slurry;

(b) calculate the contaminant concentrations and counting rates of the

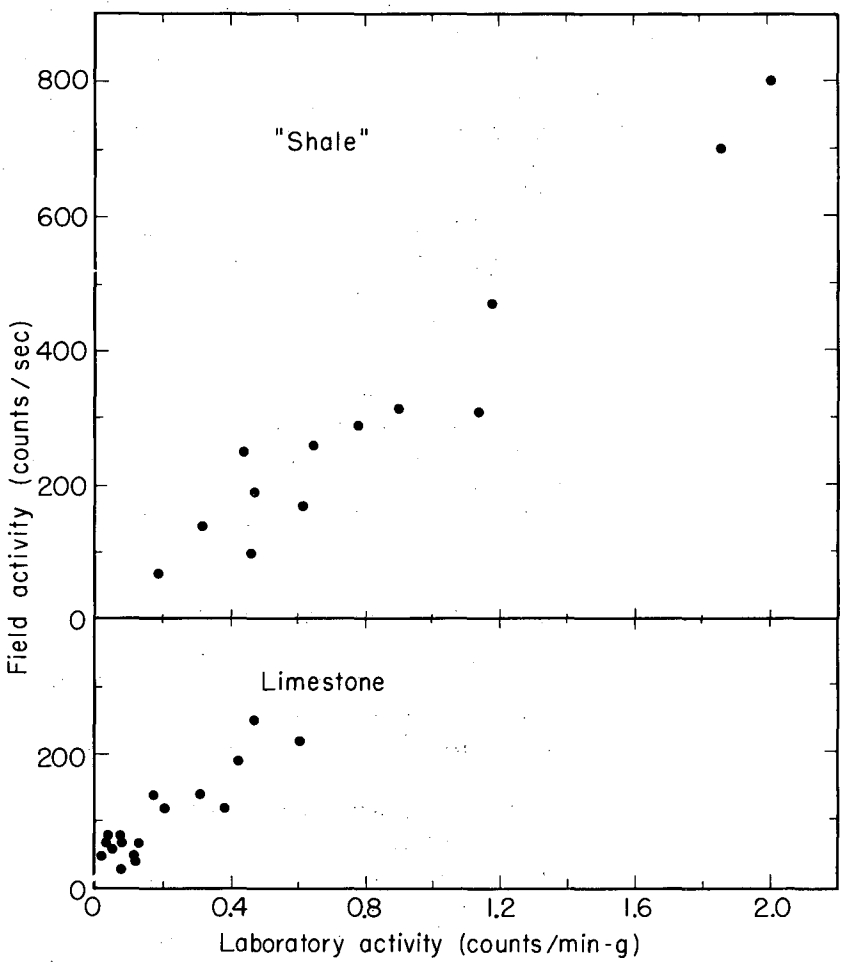

Field vs laboratory counting rates for limestone and cement-plant "shale" samples

MU-29929

Fig. 15

Table VIII. Average counting rates for cements derived from the most utilized limestones

Limestone formation	Geographic location	No. of plants reporting	Cement average counting rate (counts/min-g)
Oyster shells	Gulf and West Coasts	5	0.416
Jacksonburg	Lehigh Valley, Pa.	6	0.478
Conosauga	Alabama and Georgia	3	0.541
Becraft, Coeymans, N. Scotland and Manilius	Appalachian region, Va. to Catskill Mts., N. Y.	5	0.524
Rogers City	Wisc., Mich., and northern N. Y.	4	0.680
Vanport	Western Pa. and eastern Ohio	4	1.100
Austin Chalk	San Antonio and Dallas, Texas	2	0.692
Iola	Eastern Kansas	2	0.800
Metaline	Northeastern Wash.	2	0.594
Annona Chalk	Central Arkansas	2	0.635

clinkerized ingredients by dividing measured U, Th, K, and counting-rate values for each slurry component by 100% minus respective ignition loss;

(c) calculate finished product's U, Th, and K concentrations and the overall counting rate by weighting values from Step (b) above by percentage compositions of the raw materials in the clinker;

(d) compare hypothetical cement values to measured values from a sample of Type I cement; this shows excellent agreement, verifying the calculation procedure and the assumptions used in the process.

Table IX. Measured and calculated radioisotope-concentrations and counting rates for a Type I cement.

Ingredient	% of slurry (by weight)	Measured contaminant concentrations in slurry ingredients			Measured overall counting rate in slurry ingredients, counts/min-g	% of clinker + gypsum (by weight) calculated from ignition loss	Calculated contaminant concentration in clinker ingredients			Calculated overall counting rate in clinker ingredients (counts/min-g)
		K (%)	U (ppm)	Th (ppm)			K (%)	U (ppm)	Th (ppm)	
Limestone, Hi Titer	54	0.04	1.50	0.33	0.216 (0.350 with fallout)	46	0.04	2.58	0.57	0.372
Limestone, Lo Titer	29	0.13	1.59	0.26	0.238 (0.463 with fallout)	27	0.13	2.56	0.42	0.384
Tailings	10	0.85	1.07	1.25	0.335 (0.402 with fallout)	15.5	0.85	1.10	1.29	0.345
Dunsmuir Shale	4	1.05	1.82	4.24	0.619 (1.003 with fallout)	6	1.05	1.98	4.60	0.673
Cassidy shale (60% combustible)	3	0.41	0.55	1.65	0.220 (0.248 with fallout)	1.5	0.41	1.83	5.50	0.734
Gypsum	--	--	--	--	--	4	0.05 (measured)	0.35 (measured)	0.13 (measured)	0.059 (0.076 with fallout)
		Weighted totals for slurry (calculated)					Weighted totals for clinker and gypsum (calculated)			
		0.20	1.35	0.57	0.233		0.20	2.09	0.92	0.367
					Measured Type I cement		0.18	2.17	0.93	0.365 (0.412 with fallout)

VII. CONCLUSION

We have described both field and laboratory techniques for evaluation of the gamma-ray component of environmental radiation; some applications for these techniques have been cited.

Laboratory analysis enables us to make quantitative assay for potassium, uranium, and thorium. Radiometric assay for potassium agrees well with chemical methods. Our assays for uranium and thorium are based only on the NBL calibration ores, and have not been checked against chemical methods. Such cross-calibrations need to be performed. In addition, we need to try our assay methods on samples that have been assayed by other workers. We should like to hear from those of you who would be willing to contribute such samples for our tests.

Valid uranium and thorium assays require that the decay series have reached secular equilibrium. We have not made thorough study of the errors introduced by lack of equilibrium. The relative insolubility of thorium and half-lives of its decay series suggest that lack of equilibrium is unlikely here. However, uranium can be leached from its host material, there are long half-lived decay members, and the gaseous member can be lost to the air--three conditions which may lead to lack of equilibrium. Most of the uranium-series gamma-rays come from daughters of radium; therefore, some of our assays may really reflect only radium content. This situation would seem most likely to occur with soil samples; we are aware of these items, but have not studied them thoroughly enough to know the real extent of the problems they pose.

A. Further Studies

Until now, successful low-background shielding has been our principal goal. Recently, the Lawrence Radiation Laboratory has given us permission to expand our studies beyond the scope of low-background shielding to encompass the applications of gamma spectroscopy to the earth sciences and the study of the relationship between the gamma radiation of natural raw materials and manufactured products.

1. Studies in Geoscience

A project of particular interest to us is the application of gamma-ray spectrographic determinations of natural radioisotopes in the study of heat generation in the earth's crust, heat flow, and rock metamorphism. Verhoogen (1956) and Birch (1954) present good synopsis and bibliographies on recent and past earth-heat studies. Presently there is active investigation (Lachenbruch, et al., 1963) dealing with the flow of heat from and through the earth's mantle and crustal layers whereby it may be determined whether the earth is gaining or losing heat. An attempt is also being made to establish the quantity of heat being transmitted from the earth's interior to the crust. Though heat transmission to the crust cannot be measured, it can be calculated if the crustal heat flow and heat generated by radioactivity are known.

Contemporary heat generation data is also valuable in determining the heat generation, rapidity of heating, and maximum temperature attained in a sequence of rocks formerly buried at great depths. Metamorphosed rocks,

particularly the blueschists of the Franciscan Formation of the California Coast Ranges, are ready subjects for such a study. The Franciscan blueschists are considered by Bailey, et al. (to be published) to have been formed in an environment of abnormally high pressure relative to the temperature. Such low temperatures can result from rapid accumulation and burial, or from abnormally low radioactivity in the rock. The parent material for the schists, Franciscan graywacke, generally contains little or no K-feldspar (Bailey and Irwin, 1959); it is possible that they are also low in other K minerals as well as U and Th.

With a sufficient concentration of radioactivity, the blueschists, if they remain in their environment of formation, should gradually be heated, converting them to the higher grade of regional metamorphism, the greenschist facies. The Franciscan blueschists have not converted; a knowledge of their radioisotope concentrations would indicate whether low radioactivity is responsible.

We are presently embarking on studies in conjunction with members of the U. S. Geological Survey where field and laboratory gamma radiation data will be applied to such problems in crustal heating and regional metamorphism.

2. Studies of Structural Materials

Besides continuing the investigation of cement raw-materials, we have proposed that an investigation of steel should also be of interest. Iron ores which we have examined contain appreciable radioactivity, yet, in most cases the finished-product steel is low in activity. Sampling and subsequent spectral analysis of the raw materials and products of the various stages of the steel-making process, e. g., blast furnace slag, open hearth furnace slag, and mill scale would document the purging of the initial radioactivity and also might furnish some insight into natural processes.

Our work will be carried on within the framework of the Health Physics Department at UCLRL, Berkeley, utilizing our recently-constructed low-background concrete counting facility. We mean to pursue this work on a full-time basis, and, in this respect, would very much like to establish and maintain contact with those of you who are also working in these areas. Such an interchange of information and ideas will certainly be mutually beneficial.

REFERENCES

*Work done under the auspices of the U. S. Atomic Energy Commission.

Adams, J. A. S. (1954), Uranium and Thorium Contents of Volcanic Rocks, Sec. 2.2 in Nuclear Geology (John Wiley and Sons, New York).

Adams, J. A. S., and C. E. Weaver (1958), Thorium-to-Uranium Ratios as Indicators of Sedimentary Processes, Bull. Am. Assoc. Petrol. Geologists 42, 387.

Ahrens, L. H., W. H. Pinson, and M. M. Kearns (1952), Association of Rubidium and Potassium and their Abundance in Common Igneous Rock and Meteorites; Geochim. Cosmochim. Acta 2.

Ahrens, L. H. (1954), The Abundance of Potassium, Ch. 3 in Nuclear Geology (John Wiley and Sons, New York).

Bailey, E. H. and W. P. Irwin (1959), K-Feldspar Content of Jurassic and Cretaceous Graywackes of Northern Coast Ranges and Sacramento Valley, California; Bull. Am. Assoc. Petrol. Geologists 43, No. 12.

Bailey, E. H., W. P. Irwin, and E. L. Jones, Franciscan and Related Rocks and their Significance in the Geology of the California Coast Ranges; to be published as a Bulletin of the California Division of Mines and Geology.

Bell, K. G. (1954), Uranium and Thorium in Sedimentary Rocks, Sec. 2.3 in Nuclear Geology (John Wiley and Sons, New York).

Birch, F. (1954), Heat from Radioactivity, Ch. V in Nuclear Geology (John Wiley and Sons, New York).

Cavell, I. W. and C. O. Peabody (1961), The Winfrith District Gamma Survey, AEEW-R-62, Radiological and Safety Division, Atomic Energy Establishment, Winfrith, Dorchester, Dorset.

Daly, R. A. (1933), Igneous Rocks and the Depths of the Earth (McGraw-Hill Book Company, Inc., New York).

Davis, G. L. and H. H. Hess (1949), Radium Content of Ultramafic Igneous Rocks, II: Geological and Chemical Implications, Am. J. Sci. 247, pp. 856-882.

Evans, R. H. and H. Williams (1935), The Radium Content of Lavas from Lassen Volcanic National Park, California, Am. J. Sci. 5, No. 29.

Frondel, C. (1956), Minerology of Thorium; Geol. Survey Prof. Paper 300.

Goldsworthy, W. W. (1960), Transistorized Portable Counting-Rate Meter, Nucleonics, 18, No. 1, pp. 92-99.

Gregory, A. F. and J. L. Horwood (1961), A Laboratory Study of Gamma-Ray Spectra at the Surface of Rocks, Mines Branch Research Report R-85, Dept. of Mines and Technical Surveys, Ottawa.

Keevil, N. B. (1944), Thorium-Uranium Ratios in Rocks and Minerals; Am. J. Sci. 242, pp. 309-321.

Koczy, F. F. (1954), Geochemical Balance in the Hydrosphere, Sec. 2.4C in Nuclear Geology (John Wiley and Sons, Inc., New York).

Lachenbruch, A. (1963), private communication, U. S. Geological Survey, Menlo Park, California.

Larsen, E. S., G. Phair, D. D. Gottfried, and W. L. Smith (1956), Uranium in Magmatic Differentiation, U. S. Geol. Survey Prof. Paper 300.

Lowder, W. M., W. J. Condon, and H. L. Beck (1963), Field Spectrometric Investigations of Environmental Radiation in the U. S. A., Proceedings of the International Symposium on Natural Radiation Environment.

Patterson, H. W., W. N. Hess, B. J. Moyer, and R. W. Wallace, (1959), The Flux and Spectrum of Cosmic-Ray-Produced Neutrons as a Function of Altitude, Health Phys. 2., pp. 69-72.

Petterson, H. (1954), Radioactive Elements in Ocean Waters and Sediments, Sec. 2.4a in Nuclear Geology (John Wiley and Sons, Inc., New York).

Rankama, K. (1954), Isotope Geology, (Pergamon Press, Ltd., London).

Rankama, K. and T. Sahama (1950), Geochemistry; (University of Chicago Press, Chicago).

Verhoogen, J. (1956), Temperatures Within the Earth, Ch. 2 of Physics and Chemistry of the Earth, Vol. I, (Pergamon Press, Ltd., London).

Williams, H. (1957), Geologic Map of the Central Part of the High Cascade Range, Oregon; (map with accompanying text published by the Oregon Department of Geology and Mineral Industries, Corvallis, Oregon).